# Tracking the tempo of a continental margin arc: Insights from a forearc succession in West Antarctica

Teal R. Riley[1,†], Michael J. Flowerdew[2], Andrew Carter[3], Michael L. Curtis[2], Ian L. Millar[4], J. Alistair Crame[1], and Martin J. Whitehouse[5]

[1]*British Antarctic Survey, High Cross, Madingley Road, Cambridge CB3 0ET, UK*

[2]*CASP, Madingley Rise, Madingley Road, Cambridge CB3 0UD, UK*

[3]*Department of Earth and Planetary Sciences, Birkbeck, University of London, Malet Street, London WC1E 7HX, UK*

[4]*British Geological Survey, Keyworth, Nottingham NG12 5GG, UK*

[5]*Swedish Museum of Natural History, Box 50007, SE-104 05 Stockholm, Sweden*

## ABSTRACT

The Fossil Bluff Group of eastern Alexander Island records the exceptional preservation of more than 8 km of Mesozoic sedimentary rocks deposited into an accretionary forearc basin that developed unconformably above a late Paleozoic accretionary complex, and in proximity to a continental margin arc during a prolonged phase of enhanced magmatism. Through the Mesozoic, the Fossil Bluff Group evolved from a trench-slope environment to a forearc basin sourced from the continental margin arc. During this period, the Antarctic Peninsula's convergent margin was characterized by episodes of magmatic flare-ups that developed during tectonic compression, crustal thickening, extension, and uplift. U-Pb and Lu-Hf detrital zircon data are used to determine the provenance of the forearc succession and as a monitor of arc magmatic tempos during the late Mesozoic. The magmatic record in the adjacent arc is poorly preserved or partially absent, but the sedimentary record of the forearc basin preserves a largely uninterrupted record of arc magmatism that can be studied with detrital zircon geochronology and geochemistry. The basal succession of the Fossil Bluff Group is sourced from the adjacent accretionary complex, but thereafter it is strongly controlled by the proximal arc in western Palmer Land and is characterized by a mixed arc/recycled signature during episodes of renewed sedimentation. However, the main phases of deposition during the Early Jurassic (ca. 180 Ma), Early Cretaceous (141–131 Ma), and mid-Cretaceous (125–102 Ma) are dominated by arc-only sources. The Lu-Hf isotopic record supports a transition from convergence to extension and a return to convergence during the Mesozoic, which is consistent with accretionary orogens from elsewhere along the West Gondwanan margin. The provenance record during the depositional history of the basin points overwhelmingly to an autochthonous origin; as such, models for parts of the western province of the Antarctic Peninsula being allochthonous are unsupported.

## 1. INTRODUCTION

The Mesozoic Fossil Bluff Group of the Antarctic Peninsula preserves the accumulation of >_8 km of arc-derived material into a forearc basin that developed unconformably above a late Paleozoic–Mesozoic accretionary complex (LeMay Group). The Fossil Bluff Group is exposed along the eastern margin of Alexander Island (Figs. 1–3) in a narrow, ~250-km-long belt. The forearc succession of Alexander Island is interpreted to continue north (Fig. 1) into Adelaide Island (Riley et al., 2012) and the South Shetland Islands (Bastias et al., 2023) and potentially forms components of the Magallanes- Austral Basin (Dobbs et al., 2022), although the geology is mostly obscured. The succession has a depositional history from the Early Jurassic to the mid-Cretaceous and forms one of the most complete ancient forearc successions in the world (Doubleday et al., 1993). However, despite many authors having investigated the lithostratigraphy (e.g., Butterworth et al., 1988), fossil record (e.g., Crame and Howlett, 1988), and tectonic development (e.g., Storey et al., 1996), the origin of the basin and its provenance remains uncertain. Addressing these aspects is central to understanding the tectonic and mag-

matic history of the West Gondwanan margin, its subsequent break-up, and the formation of the Antarctic Peninsula.
Vaughan and Storey (2000) interpreted Alexander Island as a possible exotic terrane (Western Domain; Fig. 1) that accreted to the Antarctic Peninsula during the Early to mid- Cretaceous. This was a period of global plate reorganization (Matthews et al., 2012) and coincided with an Early to mid-Cretaceous magmatic “flare-up” event in the Antarctic Peninsula (Riley et al., 2018) that can be traced from Patagonia (Pankhurst et al., 1999) through West Antarctica (Siddoway et al., 2005) and New Zealand (Milan et al., 2017). Vaughan et al. (2012) identified a pronounced mid-Cretaceous compressional event that led to deformation and terrane translation along the West Gondwanan margin (Vaughan and Storey, 2000; Vaughan et al., 2002; Guenthner et al., 2010; Riley et al., 2023). Commenting on the deformational history of the Fossil Bluff Group, Nell and Storey (1991) suggested that strike-slip motion along the LeMay Range Fault, which separates the LeMay Group accretionary complex from the Fossil Bluff Group forearc succession (Fig. 2), had a long history. The LeMay Range Fault initially formed as a dextral strike-slip fault owing to the oblique subduction of the Phoenix Plate. These conditions are conducive to the translation of forearc slivers and terrane displacement (Jarrard, 1986). Therefore, a key question is whether the Fossil Bluff Group succession was deposited in situ. Recent contributions have tended to favor an in situ continental arc setting (Burton-Johnson and Riley, 2015; Gao et al., 2021; Bastias et al., 2021), although Riley et al. (2023) suggested a para-autochthonous origin for at least parts of the western margin of the Antarctic Peninsula, with accretion developing after 90 Ma.

To explain more about the origin of the Fossil Bluff Group and the contemporaneous magmatic history of the adjacent arc, this study examined the detrital zircon U-Pb record of the forearc succession from basal units overlying the LeMay Group accretionary complex to the uppermost sequences along the eastern margin of Alexander Island. Using U-Pb zircon age profiles and Lu-Hf isotopes, we investigated the source of material into the forearc basin and evaluated the likely depositional age of the succession and basin formation. Evaluating the complete record of the forearc basin through the late Mesozoic allows a more detailed understanding of the magmatic evolution of the continental margin arc and episodes of uplift and erosion. The new detrital zircon geochronological data has allowed us to produce an updated geological map of the entire Fossil Bluff Group and refine the boundaries between different formations (Fig. 3).

## 2. GEOLOGICAL SETTING

### 2.1. Antarctic Peninsula

The Antarctic Peninsula has a geological history that extends back to the Ordovician (Fig. 1) and is marked by a series of magmatic tectonic, and depositional events that developed in an accretionary continental margin setting in West Gondwana (Smellie, 2021). Vaughan et al. (2002) suggested that the Antarctic Peninsula developed through a process of terrane translation and accretion onto the West Gondwanan margin, although more recent contributions favor an autochthonous continental arc setting (e.g., Bastias et al., 2021).

### 2.2. Alexander Island

The geology of Alexander Island (Fig. 2) can be divided into four geological units: (1) a late Paleozoic–early Mesozoic accretionary complex (LeMay Group; Riley et al., 2023) in unconformable/faulted contact with (2) a shallowing forearc basin/trench slope sedimentary succession at least 8 km in thickness (Fossil Bluff Group; this study). The LeMay Group is intruded by (3) Late Cretaceous–Cenozoic granites, and locally overlain by volcanic units of the same age (McCarron and Millar, 1997). (4) The final geological unit on Alexander Island is an episode of Neogene–Quaternary (7–0.1 Ma) alkaline volcanism that erupted following the end of subduction; it forms two separate volcanic fields in northern and southwestern Alexander Island (Fig. 2) that are part of the Bellingshausen Sea volcanic field (Smellie and Hole, 2021).

Vaughan and Storey (2000) interpreted Alexander Island as either a subduction-accretionary complex to the para-autochthonous/allochthonous Central Domain (Fig. 1) or as an allochthonous exotic terrane (Western Domain; Fig. 1) that “docked” with the Antarctic Peninsula during the mid-Cretaceous Palmer Land Event (Vaughan et al., 2012). Collision with the Antarctic Peninsula may have occurred farther south than its current position, with continental margin parallel translation taking place along a large-scale dextral shear zone (Vaughan and Storey, 2000). There are several advantages to a segmented model for the Antarctic Peninsula and an allochthonous Central-Western Domain. Subduction geometry and granitoid chemistry for Antarctic Peninsula Mesozoic magmatism is more straightforward to explain with a trench closer to Palmer Land, as opposed to a greater lateral distance when the Central-Western Domain occupies its current position (Bastias et al., 2023). Also, a terrane translation model for the Antarctic Peninsula is consistent with mid-Cretaceous tectonic models elsewhere along the West Gondwanan margin (e.g., New Zealand; Robertson et al., 2019). However, an allochthonous model for the Central-Western Domain with a mid-Cretaceous suturing is difficult to reconcile with certain aspects of geochronology and aeromagnetic data across putative terrane boundaries (Burton-Johnson and Riley, 2015). In this paper, we examine the juxtaposition between Alexander Island and the Antarctic Peninsula and the relationship between the LeMay Group and Fossil Bluff Group and arc magmatism of Palmer Land, and whether a suspect terrane model is appropriate for the Western Domain.

The deformational history of the forearc succession has been investigated by Doubleday and Storey (1998), who examined successions from the Middle Jurassic to the mid-Cretaceous. They identified three distinct deformational events: (1) Middle Jurassic strike-slip movement on the LeMay Range Fault (Fig. 2) in the accretionary complex; (2) forearc basin inversion in the mid-Cretaceous that developed in a dextral transpressional setting; and (3) post-inversion extension, which was the final deformational phase, and postdates the depositional history of the Fossil Bluff Group; this phase led to the opening of the George VI Sound rift (Fig. 2). Doubleday and Storey (1998) attributed phase 1 to be related to oblique subduction, while basin inversion (phase 2) was a Pacific-wide, mid-Cretaceous compressional event. This is consistent with calculated convergence rates in Riley et al. (2020a) and Burton-Johnson et al. (2022), which demonstrated an increase in convergence post-140 Ma. The later transtensional phase of deformation was interpreted by Nell and Storey (1991) to be related to oblique subduction after 50 Ma, or potentially due to ridge segment–trench collision that resulted in the cessation of subduction at ca. 30 Ma (Larter and Barker, 1991). However, Jordan et al. (2014) determined that arc magmatism on Adelaide Island continued until at least ca. 23 Ma. This later event was highlighted by Twinn et al. (2022), who identified an episode of accelerated cooling at ca. 25 Ma (apatite thermochronometry) that was associated with trench collision of a spreading ridge segment.

### 2.3. Fossil Bluff Group and Sample Information

The forearc basin clastic sedimentary succession of the Fossil Bluff Group unconformably overlies, and is in faulted contact with, the accretionary LeMay Group (unit 1 in Fig. 3). There are several localities west of Planet Heights (Fig. 3) where rocks of the Fossil Bluff Group rest unconformably on the LeMay Group (Edwards, 1979; Tranter, 1987). At the boundary between the two groups, it is evident that the LeMay Group was deformed prior to deposition of the Fossil Bluff Group (Storey and Nell, 1988), while elsewhere the boundary is a major fault (LeMay Range Fault; Edwards, 1979).

The Fossil Bluff Group was initially defined by Butterworth et al. (1988), but has been revised several times and is now defined as an ~8 km succession of clastic units that record a transition from trench slope to forearc basin deposition as part of a major shallowing sequence. At least 11 separate, mappable units have been identified across the Fossil Bluff Group (Fig. 3), with deposition likely to extend from the Bajocian (ca. 170 Ma) to the Albian (ca. 100 Ma)

based on biostratigraphy and lithostratigraphy (e.g., Doubleday et al., 1993; Crame and Francis, 2024), although the main phase of forearc deposition probably developed through the mid-Cretaceous. The forearc succession is best defined as a compressional accretionary basin with landward migration of the depo-center (cf. Noda, 2016) and episodes of extension. The geological map of the Fossil Bluff Group is shown in Figure 3 with the depositional age primarily constrained by molluscan fossils and plant material (Butterworth et al., 1988), but it was adapted following the analysis presented here.

Samples for detrital zircon (U-Pb and Lu-Hf) analysis were selected from across the Fossil Bluff Group (Fig. 2) to examine their provenance through the entire depositional history of the succession. Fifteen samples were selected for analysis from eastern Alexander Island, with samples from the lowermost Selene Nunatak Formation and uppermost Neptune Glacier Formation included (Fig. 3). Several samples were also examined from the basin-wide Himalia Ridge Formation. A detailed and revised geological map and sample locations are shown in Figure 3. Precise positional information is provided for all samples in Table S1 in the Supplemental Material1.

The lowermost succession of the Fossil Bluff Group is the Selene Nunatak Formation (unit 2 in Fig. 3), which forms a narrow north-south–trending unit in the central part of the succession (Fig. 3). The sequence is ~150 m in thickness, with the type section defined from Selene Nunatak (Fig. 3), where the unit unconformably overlies the accretionary complex of the LeMay Group (unit 1 in Fig. 3). The Selene Nunatak Formation is characterized by pebble-cobble conglomerate (sedimentary clasts) that is associated with laminated mudstones and coarser units (Doubleday et al., 1993). Two samples for detrital zircon analysis were selected from the Selene Nunatak Formation from the western end of Nonplus Crag, north of the type locality at Selene Nunatak (Fig. 3). Samples KG.4640.33 and KG.4640.44 are medium- to coarse-grained sandstones, which have a weakly developed structural fabric.

The Atoll Nunataks Formation (unit 3 in Fig. 3) conformably overlies the Selene Nunatak Formation and forms a sequence ~1000 m in thickness, with its type section exposed to the east of Atoll Nunataks (Fig. 3). Holdsworth and Nell (1992) interpreted the Atoll Nunataks Formation as a trench-slope sequence that dips beneath parts of the forearc basin and may pre-date the formation of the “true” forearc succession. The Atoll Nunataks Formation dips moderately to the east and has no penetrative fabric, although the sequence is characterized by irregular fractures and joints. Sample KG.3669.24, near Lunar Crag (Fig. 3), is from a coarse-grained sandstone interbed with small sedimentary pebble clasts.

The Ablation Point Formation (unit 4 in Fig. 3) is confined to the eastern margin of Alexander Island between Jupiter Glacier and Belemnite Point (Taylor et al., 1979), with the type section defined from Ablation Point (Fig. 3). At Ablation Point, the sequence has a minimum thickness of 350 m, but reaches a thickness of 440 m at the nearby Himalia Ridge (Fig. 3). The Ablation Point Formation comprises a zone of highly disturbed and brecciated sediments, which have been interpreted as a syn-sedimentary mélange (Macdonald and Butterworth, 1986). Sample KG.3657.4 is a medium-grained sandstone from a sandstone-mudstone interbed adjacent to a minor thrust fault. The unit is host to poorly preserved perisphinctid ammonites. The extent of the Ablation Point Formation is also interpreted to continue across King George VI Sound into northwest Palmer Land (Taylor et al., 1979) at Carse Point, where sandstone sample R.2151.30 is located (Fig. 2).

The Himalia Ridge Formation (unit 5; Fig. 3) is the only unit of the Fossil Bluff Group that is basin-wide, with the type section defined from Himalia Ridge (Fig. 3), where a maximum thickness of ~2600 m has been recorded, although elsewhere, the Himalia Ridge Formation has a thickness in the range of 1000–1500 m (Butterworth et al., 1988).

The Himalia Ridge Formation has a variable stratigraphy and is characterized by a broad range of different facies with considerable lateral variation. The unit consists of four major conglomerate beds that form prominent steep scarps. The conglomerate beds are 80–170 m in thickness (Miller and Macdonald, 2004) and are channeled with westward paleoflow indicators that suggest a source direction from the magmatic arc to the east. At its type section, three distinct pulses of coarse-grained sediment input have been recognized, which are interpreted to reflect tectonic allocyclic control and to be related to uplift in the hinterland (Butterworth, 1991). Significant arc uplift is also supported by a shift in conglomerate clast composition from volcanic to plutonic. This is also reflected in the sandstone petrofacies that trend from undissected arc to dissected arc/basement uplift, which Butterworth (1991) attributed to arc unroofing.

Macdonald et al. (1999) identified oceanic-island basalt–like rocks that were contemporaneous with the deposition of the Himalia Ridge Formation and were used as evidence of a dynamic rift-setting for forearc basin development.

In the upper part of the Himalia Ridge Formation, the Jupiter Glacier Member (unit 5a in Fig. 3) crops out at Callisto Cliffs and consists of fine-grained, laminated sandstones that represent an abrupt, but temporary, regional shallowing event.

Three samples were analyzed from the Himalia Ridge Formation and were collected from the Ganymede Heights–Ablation Valley area (Fig. 3). Samples KG.2883.4 and KG.3069.2 from Ablation Valley are medium- to coarse-grained sandstones that crop out above a minor thrust zone. Sample KG.3463.3 is a collection of several granitoid cobbles from a conglomerate bed at Ganymede Heights.

The Spartan Glacier Formation (unit 6 in Fig. 3) is ~1 km in thickness, and its type locality crops out to the south of Spartan Glacier (Butterworth et al., 1988). The formation is characterized by mudstone and siltstone with minor, fine-grained sandstone interbeds. The Spartan Glacier Formation is host to a broad molluscan fauna, but is not particularly age diagnostic, although an Early Cretaceous (Berriasian–Hauterivian) age is suggested (Crame and Howlett, 1988).

There is a clear transition from the uppermost Himalia Ridge Formation/Jupiter Glacier Member to the Spartan Glacier Formation in terms of sediment supply, which shifts from clastic gravels to fine-grained lithologies. Butterworth (1991) determined that the Spartan Glacier Formation was deposited in a tectonically quiescent setting, although slope-collapse deposits and local angular unconformities indicate some tectonic control.

Two samples were analyzed from the Spartan Glacier Formation (unit 6). Sample KG.3231.2, from Leda Ridge (Fig. 3) near Ganymede Heights, is a medium-grained graded sandstone, while KG.3968.2 is from a narrow band of the Spartan Glacier Formation near Offset Ridge (Fig. 3) and is a siltstone/fine-grained sandstone.

The Pluto Glacier Formation (unit 7 in Fig. 3) is exposed extensively across the southern sector of the Fossil Bluff Group and has a total thickness of up to 2500 m (Moncrieff and Kelly, 1993). The succession is characterized by a high proportion proportion of fine- to medium-grained sandstones that are locally cross-bedded and bioturbated (Moncrieff and Kelly, 1993). The Pluto Glacier Formation is an extensive shelf sandstone/deltaic unit that may have a diachronous relationship with deltaic and terrestrial sequences farther south (Butterworth, 1991).

The Rhea Corner Member (unit 7a) is a distinct unit in the Pluto Glacier Formation and occurs in the upper part of the succession at Rhea Corner (Fig. 3). It forms a 370-m-thick sandy and

conglomeratic unit, with a strongly erosive base, and contrasts with the dominantly finer grained lithology of the Pluto Glacier Formation.

Three samples were analyzed from the Pluto Glacier Formation (unit 7). Sample KG.3969.1, near Astarte Horn (Fig. 3), is adjacent to the contact with the LeMay Group accretionary complex. The sample is a cross-bedded, coarse siltstone from a reverse faulted slice of the Pluto Glacier Formation in faulted contact with the LeMay Group. Sample KG.3959.2 is a medium-grained sandstone bed from the Pluto Glacier Formation at Offset Ridge (Fig. 3), while KG.4109.1 is a medium-grained and well-bedded sandstone from Pickering Nunataks (Fig. 3).

The uppermost 2500 m of the Fossil Bluff Group forms the Neptune Glacier Formation, which has been split into three separate units (Fig. 3). The Deimos Ridge Member (unit 8 in Fig. 3) crops out south of the Venus Glacier and forms a 700-m-thick succession of predominantly sandstone with mudstone interbeds. The Milestone Bluff Formation of central Adelaide Island, ~120 km north of Alexander Island (Fig. 1), forms a succession at least 1500 m in thickness of sandy, turbiditic sedimentary units with minor interbedded crystal and vitric tuff units and has been correlated to the Deimos Ridge Member (Riley et al., 2012). Cobble and boulder conglomerates form prominent units of up to 20 m in thickness, and clast orientations suggest a source to the east. Riley et al. (2012) dated a crystal tuff bed from the Milestone Bluff Formation at 113.9 ±1.2 Ma.

One sample was examined here to investigate the potential correlation of the Alexander Island and Adelaide Island sectors of the forearc basin. Sample J6.288.2 is a matrix-supported pebble conglomerate (dominantly volcanic clasts) from Milestone Bluff (Fig. 1).
The Triton Point Member (unit 9; Fig. 3) has a total thickness of ~800 m and crops out at Triton Point and farther south at Coal and Titan nunataks, where the unit is thickest (Nichols and Cantrill, 2002). It is characterized by standing trees at the base of the succession and marine fauna from near the top, which support a late Albian age (Crame and Howlett, 1988). Sample KG.4956.1 is a coarse-grained sandstone bed from the upper part of an ~700-m-thick succession at Coal Nunatak. There is an abrupt change in facies from the Deimos Ridge Member to the Triton Point Member, with an erosion surface marking the base of a braided fluvial channel sandstone unit. Uplift prior to the incised river channels led to subaerial conditions, and plant roots are evident (Nichols and Cantrill, 2002). Paleocurrent evidence from Moncrieff and Kelly (1993) and Nichols and Cantrill (2002) demonstrates sediment input from the arc to the east, but transport to the southwest in the south and to the northwest in the north, which developed across a braided plain delta extending ~30 km to the north and west. The uppermost unit of the Fossil Bluff Group is the Mars Glacier Member (unit 10 in Fig. 3), which crops out from Triton Point to Two Step Cliffs (Fig. 3). This unit forms a sequence of up to 1000 m in thickness and is dominated by medium-grained sandstones with subordinate mudstones and conglomerates and is characterized by fossil forest horizons (Nichols and Cantrill, 2002). No samples were examined from the Mars Glacier Member as part of this study.

## 3. ANALYTICAL METHODS

### 3.1. U-Pb Zircon Geochronology

Zircon (U-Pb) geochronology was conducted at the Swedish Museum of Natural History and University College London. Full analytical procedures, data (Table S2), and cathodoluminescence images (Fig. S1) from each laboratory are provided in the Supplemental Material, but a summary of the analytical procedures is provided here.

At the Swedish Museum of Natural History (Stockholm), U-Pb ion-microprobe zircon geochronology was conducted using a CAMECA 1280 ion microprobe at the NordSIMS facility. The analytical method closely followed Whitehouse and Kamber (2005) but differs insomuch

that the oxygen ion primary beam was generated using a high-brightness, radiofrequency (RF) plasma ion source (Oregon Physics Hyperion II, rather than a duoplasmatron) and a focused beam instead of an illuminated aperture. The 10 nA O2-beam was rastered over 5 × _5 μm to homogenize beam density, and the final analytical spot size was ∼15 μm in diameter. Sputtered secondary ions introduced into the mass spectrometer were analyzed using a single ion-counting electron multiplier over 10 cycles of data. Data were reduced using software developed in-house. The power law relationship between 206Pb/238U16O and 238U16O2/238U16O measured from the 91500 standard was used to calibrate U/Pb ratios following the recommendations of Jeon and Whitehouse (2015). Common-Pb corrections were applied to analyses where statistically significant 204Pb was detected, using the present-day terrestrial common-Pb estimate of Stacey and Kramers (1975). 207Pb-corrected ages were calculated assuming non-radiogenic Pb was from surface contamination and had an isotopic composition of modern-day average terrestrial common Pb (207Pb/206Pb =_ _0.836; Stacey and Kramers, 1975).

Zircon U-Pb geochronology at University College London was conducted using laser ablation–inductively coupled plasma–mass spectrometry (LA-ICP-MS; an Agilent 7700 coupled to a New Wave Research 193 nm excimer laser) at the London Geochronology Center. Typical laser spot sizes of 25 μm were used with a 7–10 Hz repetition rate and a fluence of 2.5 J/cm2. Background measurement before ablation lasted 15 s, and the laser ablation dwell time was 25 s. The external zircon standard was Plešovice, which has a thermal ionization mass spectrometry (TIMS) reference age of 337.13 ± _0.37 Ma (Sláma et al., 2008). Standard errors on isotopic ratios and ages include the standard deviation of 206Pb/238U ages of the Plešovice standard zircon. Time-resolved signals that record isotopic ratios with depth in each crystal were processed using GLITTER 4.5 data reduction software developed by the ARC National Key Center for Geochemical Evolution and Metallogeny of Continents (GEMOC) at Macquarie University and the Commonwealth Scientific and Industrial Research Organisation (Australia) Exploration and Mining division. Processing enabled filtering to remove spurious signals resulting from overgrowth boundaries, weathering, inclusions, and fractures. Ages were calculated using the 206Pb/238U ratios for samples dated as younger than 1.1 Ga and the 207Pb/206Pb ratios for older grains. Discordance was determined using [(207Pb/235U − _206Pb/238U)/206Pb/238U] and 207Pb/206Pb ages.

### 3.2. Lu-Hf Isotopic Analysis

Lu-Hf isotopes were determined on a subset of those samples analyzed for their U-Pb age, and analysis was conducted using the same spot as was used for U-Pb geochronology. Eight samples were selected for analysis to provide a good representation through the Fossil Bluff Group succession. The analyses were determined on a Neptune multicollector–inductively coupled plasma–mass spectrometer (MC-ICP-MS) coupled with a laser ablation system at the British Geological Survey, Keyworth, UK. Initial 176Hf/177Hf ratios were calculated using the U-Pb crystallization age of each grain, and the results are expressed as initial εHf (εHfi). εHf values were calculated using a 176Lu decay constant of 1.867 × _10–11y−1 (Söderlund et al., 2004), the present-day chondritic 176Lu/177Hf value of 0.0336, and an 176Hf/177Hf ratio of 0.282785 (Bouvier et al., 2008). Full analytical details are provided in the Supplemental Material, and the data are presented in Table S3.

## 4. RESULTS

### 4.1. U-Pb Detrital Zircon Geochronology

The age distributions of all 15 samples analyzed are plotted in Figure 4 as probability density plots (after Vermeesch, 2018) overlain with kernel density estimator curves. Overall, there is significant variation across the Fossil Bluff Group, with a clear younging age distribution toward the eastern part of the succession and certain units displaying a broader pattern of older zircon grains. Two samples (KG.4640.33 and KG.4640.44) from the Selene Nunatak Formation (unit

2) from the base of the Fossil Bluff Group have the broadest spread of detrital zircon ages (Figs. 4A and 4B) of all the analyzed samples, with a prominent Late Permian age peak at ca. 265 Ma and a significant range of ages through the Paleozoic. The age distribution, with a prominent Late Permian peak, is akin to the adjacent LeMay Group accretionary complex (Riley et al., 2023), although a younger age of deposition for the Selene Nunatak Formation is indicated by rare zircon grains that record ages younger than 220 Ma. The age distribution is characteristic of a strong local bias with a proximal source-to-sink depositional environment. The detrital zircon population is broadly consistent with a possible Bajocian biostratigraphical age for the Selene Nunatak Formation (ca. 170 Ma; Butterworth, 1991).

The sample from unit 3 (Atoll Nunataks Formation) records a very different age profile than those samples from the underlying Selene Nunatak Formation. Sample KG.3669.24 has a prominent Early Jurassic age peak of ca. 183 Ma and a secondary Triassic age peak at ca. 204 Ma (Fig. 4C). No Paleozoic age populations are identified in sample KG.3669.24, which indicates that there is no contribution from the proximal LeMay Group accretionary complex or the underlying Selene Nunatak Formation. The age profile is consistent with a likely Bajocian–Bathonian depositional age (ca. 177 Ma; Fig. S2), which places it in the lower part of the Atoll Nunataks Formation. The detrital zircon age population presented here is not in agreement with the interpretation of Doubleday et al. (1993), who interpreted that the Atoll Nunataks Formation was derived from the proximal LeMay Group accretionary complex. The complete absence of Permian zircon grains in sample KG.3669.24 of the Atoll Nunataks Formation indicates no source relationship to the LeMay Group.

The Ablation Point Formation is restricted to eastern Alexander Island, and also the western margin of northwest Palmer Land at Carse Point (Fig. 2). Two samples (KG.3657.4 and R.2151.30) from the Ablation Point Formation share very similar age profiles in the interval 217–207 Ma, characterized by prominent Late Jurassic (ca. 155 Ma) age peaks and well-defined Triassic peaks (Figs. 4D and 4E). Both samples yield maximum likely depositional ages of ca. 155 Ma (Fig. S2). The sample from north of Belemnite Peak (KG.3657.4) has a broader age profile, with zircons from the Carboniferous and Ordovician. A depositional age of ca. 155 Ma is also supported by its suspected Kimmeridgian fauna (Crame and Howlett, 1988). The age profile from the sandstone at Carse Point (sample R.2151.30) has a more localized depositional signature, with no significant regional component that is characteristic of the adjacent sample near Belemnite Point (sample KG.3657.4).

The Himalia Ridge Formation (unit 5) is basin-wide, and two samples (KG.2883.4 and KG.3069.2) from close to the type locality record very similar age profiles. Both samples have prominent Early Cretaceous age peaks of ca. 143 Ma, with a secondary peak shoulder at ca. 138 Ma (Figs. 4F and 4G), and yield maximum depositional ages of ca. 140 Ma (Fig. S2). The Himalia Ridge Formation is also characterized by a mid-Triassic signal at ca. 213 Ma, akin to the Ablation Point Formation and a peak at ca. 182 Ma that is also evident in the Atoll Nunataks Formation. Granitoid clasts from a conglomerate (sample KG.3463.2) from the Himalia Ridge Formation record a single age peak at ca. 140 Ma (Fig. 4H), which indicates likely supply from a distinct erosional level and correlates with the primary detrital zircon age peaks from the sandstone samples of the Himalia Ridge Formation. The granitoid-dominant conglomerate unit is typical of the upper part of the Himalia Ridge Formation, with its source from a deeper erosional level (Butterworth, 1991).

The Spartan Glacier Formation shares a distribution of ages similar to that of the underlying Himalia Ridge Formation. Two samples from the Spartan Glacier Formation were analyzed from almost opposite ends of the lateral extent of the unit (Fig. 3). Sample KG.3968.2 is located at the southern extent of the Spartan Glacier Formation, ~85 km south of sample site KG.3231.2. Despite the distance between sample sites, both share very similar age distribution profiles, with prominent Early Cretaceous age peaks (143–136 Ma; Figs. 4I and 4J) and a broader distribution of ages through the Early Jurassic (ca. 184 Ma) and the mid-Triassic (ca.

218 Ma). Both samples have a broad distribution of recycled zircon grains, which indicates a degree of exhumation and erosion of basement material.

Three samples from the Pluto Glacier Formation exhibit very similar age distributions (Figs. 4K–4M). Two samples (KG.3959.2 and KG.4109.6) are from the main succession of the Pluto Glacier Formation, while sample KG.3969.1 is from a reverse faulted slice farther west. All are characterized by a prominent Early to mid-Cretaceous age peak at ca. 126 Ma that constitutes ~90% of the detrital zircon population and likely indicates a depositional environment with a prominent local bias, but with a minor component of recycled basement material. This yields likely maximum depositional ages in the range of 129–124 Ma, which are broadly consistent with a Lower Aptian age (ca. 120 Ma) suggested by the molluscan fauna (Crame and Howlett, 1988), although a Barremian–Aptian age maybe more appropriate given the older maximum depositional ages.

Two samples from the uppermost Neptune Glacier Formation were analyzed, including one sample from the forearc basin extension into Adelaide Island (J6.288.2 of the Milestone Bluff Formation) and one from the Triton Peak Member at Coal Nunatak (Fig. 3; sample KG.4956.1). The detrital zircon age profiles are consistent with the stratigraphy, with sample J6.288.2 displaying two prominent Early to mid-Cretaceous age peaks at ca. 112 Ma and ca. 134 Ma (Fig. 4N), while sample KG.4956.1 is characterized by a major peak at ca. 105 Ma and a secondary peak at ca. 124 Ma (Fig. 4O). The age profiles are consistent with a local bias and no significant regional contribution from basement sources. These ages also correlate well with the biostratigraphy, which suggests deposition during the Albian.

### 4.2. Lu-Hf Isotopes

Lu-Hf isotopic analysis was conducted on a subset of the Fossil Bluff Group samples that was analyzed for U-Pb geochronology. Eight samples were selected for analysis from the Fossil Bluff Group to provide good representation across the succession. All zircon grains analyzed for U-Pb geochronology were selected for Lu-Hf analysis (Table S3). The lowermost succession analyzed was the Atoll Nunataks Formation (sample KG.3669.24), which yields εHf values in the range of −6 to 0 for the Early Jurassic age population and a tighter range (−5 to −2) for the Late Triassic population (Fig. 5A). The range for the Early Jurassic population overlaps primarily with the Latady Group sedimentary rocks (Fig. 5B) of southern Palmer Land (Fig. 1) but not with the coeval Mount Poster Formation (Fig. 1).
Two samples from the Late Jurassic Ablation Point Formation (unit 4) have a very different εHf range than the Atoll Nunataks Formation, which reflects a clear shift in source. Both samples KG.3657.4 and R.2151.30 have εHf in the range of +1 to +5, with no clear overlap with known Antarctic Peninsula magmatic events (Fig. 5).

Three samples from the Early Cretaceous Himalia Ridge Formation fall in the range of −2 to +5, but individual samples have a narrower εHf range. The granite clasts from the conglomerate bed (sample KG.3463.2) are in the range of +1 to +2, while sample KG.2883.4 is more radiogenic (−2 to +1), and KG.3069.2 is less radiogenic (>+2), despite the relative proximity of the sample sites. The Early Cretaceous population overlaps to some degree with the field for Early Cretaceous granitoids from western Palmer Land (Bastias et al., 2023). This field is likely to trend to more radiogenic values based on the εHf values of the granitoid clasts (sample KG.3463.2). Both samples KG.2883.4 and KG.3069.2 have a significant Early Jurassic (ca. 183 Ma) age population with εHf values that broadly overlap with those from the Atoll Nunataks Formation (sample KG.3669.24; Fig. 5A).
A single sample from the Early Cretaceous Pluto Glacier Formation (KG.3969.1) exhibits a relatively tight cluster of εHf values (−6 to −2) with very few older zircon grains. The mid-Cretaceous εHf values overlap with a field of Early to mid-Cretaceous granitoids examined by Bastias et al. (2023).

The youngest sample (ca. 105 Ma) investigated from the Fossil Bluff Group is KG.4956.1 from the Neptune Glacier Formation (Triton Peak Member), which shares a range in εHf val ues (+1 to +7) similar to that of the Pluto Glacier Formation. These values are akin to those of the adjacent mid-Cretaceous granitoids and volcanic rocks of northwest Palmer Land (Riley et al., 2020a; Bastias et al., 2023). A second suite of ages at ca. 125 Ma has a narrower range in εHf (−4 to −2) and overlaps with the field of granitoids associated with the Lassiter Coast intrusive suite of eastern Palmer Land (Fig. 1; Riley et al., 2018).

Also shown in Figure 5 are the Hf isotopic envelopes from West Antarctica (Nelson and Cottle, 2018). These are shown from Marie Byrd Land/Transantarctic Mountains and the Antarctic Peninsula/Thurston Island based on available data at the time. Nelson and Cottle (2018) highlighted that Phanerozoic accretionary orogens exhibit a broadly similar pattern in terms of zircon Hf isotopic evolution reflecting contraction and extension, coupled to slab boundary processes. They identified a Pacific margin-wide Cretaceous–Cenozoic isotopic “pull down” that reflects a strong lithospheric signature during contraction, which is strongly evident in the data presented here from the Fossil Bluff Group and also more recent granitoid/volcanic datasets from Palmer Land (e.g., Riley et al., 2020a; Bastias et al., 2023).

## 5. FOSSIL BLUFF GROUP PROVENANCE ANALYSIS

The U-Pb and Lu-Hf datasets from the Fossil Bluff Group of Alexander Island provide us with a framework for examining the provenance and depositional history of a long-lived forearc basin and for tracing shifts in the continental margin arc magmatism of the Antarctic Peninsula and uplift in the late Mesozoic. To evaluate the provenance history of the Fossil Bluff Group, we also examine other sedimentary successions from the Antarctic Peninsula to understand sediment recycling and source-to-sink dynamics. We compare U-Pb and Lu-Hf detrital zircon data from sedimentary rocks across the Antarctic Peninsula (Trinity Peninsula Group, Erewhon-Mount Peterson beds, Latady Group, Botany Bay Group, Mount Hill Formation, and Le May Group; Fig. 1) to the Fossil Bluff Group dataset (this study). We also consider late Mesozoic magmatism from the Antarctic Peninsula to investigate direct input from the adjacent arc into a forearc setting and to evaluate whether an autochthonous model for the Western Domain is appropriate.

### 5.1. Comparative Sedimentary Successions

#### *5.1.1. LeMay Group*

The LeMay Group is an ~4-km-thick accretionary complex that underlies, or is in faulted contact with, the Fossil Bluff Group (Fig. 2). It is a succession of variably deformed trench-fill turbidites and trench-slope sediments that are associated with mélange belts of oceanic floor material (Tranter, 1988). Riley et al. (2023) conducted a detailed examination of the provenance and depositional history of the LeMay Group and identified four separate groups. The two main groups have a Late Permian depositional age and an accretionary event in the mid-Triassic during an episode of flat-slab subduction. The other two groups (Group 3: Charcot Island, and Group 4: Mount King; Fig. 2) have considerably younger depositional ages and are not associated with the main accretionary complex. The LeMay Group was interpreted to form part of a series of Late Permian accretionary complexes and volcaniclastic successions along the West Gondwana margin (Riley et al., 2023) from South America to Australia.

#### *5.1.2. Trinity Peninsula Group*

The Trinity Peninsula Group forms part of the same suite of Late Permian–Triassic accretionary complexes that includes the LeMay Group of Alexander Island. The Trinity Peninsula Group is the dominant geological unit of the northern Antarctic Peninsula and is an ~5-km-thick succession of variably deformed siliciclastic turbidites (Hyden and Tanner, 1981). It was incorporated into an accretionary complex, possibly during the Triassic, and has been correlated with the adjacent Scotia Metamorphic Complex (Trouw et al., 1998). Several authors (e.g., Barbeau et al., 2010; Castillo et al., 2015, 2016) have examined the detrital

zircon ages of the Trinity Peninsula Group and suggested a likely Permian depositional age with links to the accretionary complexes of Patagonia.

#### *5.1.3. Erewhon Nunatak–Mount Peterson Beds*

Quartz-rich sandstones from Erewhon Nunatak and Mount Peterson in southern Palmer Land (Fig. 1) are interpreted as Late Permian based on detrital zircon analysis and *Glossopteris* flora (Elliot et al., 2016). The sandstones are distinct from the Permian accretionary complexes of the LeMay and Trinity Peninsula groups (Riley et al., 2023), and Elliot et al. (2016) interpreted them as part of a small allochthonous crustal block that is translated from its original position adjacent to the Ellsworth Mountains.

#### *5.1.4. Latady Group*

The most extensive sedimentary succession of Palmer Land is the Jurassic Latady Group, which developed in a rifted margin setting and forms a succession several kilometers in thickness. Hunter and Cantrill (2006) divided the Latady Group into five separate formations that reflect deposition in a range of settings from coastal to deep marine. U-Pb and Lu-Hf data from detrital zircons of the Latady Group were discussed by Riley et al. (2023) and highlighted a likely depositional age of ca. 183 Ma for the lower part of the succession and a Late Jurassic–Early Cretaceous depositional age for the upper part of the succession. The lower part of the Latady Group has a primary detrital zircon age peak identical to the age of the intraplate Mount Poster Formation rhyodacitic volcanic rocks (Pankhurst et al., 2000; Hunter et al., 2006) and was interpreted to form the primary source into rift-controlled basins. The upper part of the Latady Group overlaps with sections of the Fossil Bluff Group and may share common sources, which will be investigated here.

#### *5.1.5. Botany Bay Group*

The Botany Bay Group is restricted to northern Graham Land (northern Antarctic Peninsula; Fig. 1) and forms a succession of terrestrial mudstones, sandstones, and conglomerates. The Botany Bay Group is host to abundant plant fossils, which along with the detrital zircon age population (Hunter et al., 2005), suggest a Middle Jurassic depositional age (Farquharson, 1984).

#### *5.1.6. Mount Hill Formation*

The Mount Hill Formation of eastern Palmer Land (Fig. 1) was considered to be closely related to the Latady Group of southern Palmer Land (Pankhurst et al., 2000); however, only the lower Mount Hill Formation may be similar in depositional age to the upper part of the Latady Group. Detrital zircon data (Riley et al., 2023) indicate that the upper Mount Hill Formation has a considerably younger depositional age (mid-Cretaceous) and may overlap with parts of the Fossil Bluff Group succession.

#### *5.1.7. Palmer Land Cretaceous Magmatism*

Throughout the late Mesozoic, continental margin arc magmatism was widespread across large parts of the Antarctic Peninsula, particularly in Palmer Land and southern Graham Land, broadly adjacent to the forearc basin of Alexander Island. Late Mesozoic arc magmatism has been recorded from ca. 140 Ma to 90 Ma, and was punctuated by several episodes of enhanced magmatism (Riley et al., 2020a; Bastias et al., 2023). Two primary episodes of arc magmatism developed in the intervals 140–131 Ma and 126–100 Ma (Bastias et al., 2023), with a clear hiatus during the Late Jurassic–Early Cretaceous (148–140 Ma). More distal to the forearc setting is the Lassiter Coast intrusive suite of eastern Palmer Land, which preserves several pulses of granitoid magmatism through the mid-Cretaceous (130–102 Ma; Riley et al., 2018; Burton-Johnson et al., 2022).

### 5.2. Fossil Bluff Group: Interpretation

The Fossil Bluff Group of eastern Alexander Island records the exceptional preservation of >_8 km of essentially late Mesozoic sedimentary rocks deposited into an accretionary forearc basin that developed adjacent to a late Paleozoic accretionary complex and in proximity to a

continental margin arc during a phase of enhanced magmatism. During the late Mesozoic, the Antarctic Peninsula convergent margin was characterized by episodes of magmatic flare-ups that developed during tectonic compression, crustal thickening, and uplift (Burton-Johnson et al., 2022).

We used our U-Pb and Lu-Hf detrital zircon data to determine the provenance of the forearc succession and as a monitor for arc magmatic tempos during the late Mesozoic. We used multidimensional scaling (MDS) analysis to evaluate potential correlative units from the Antarctic Peninsula and elsewhere along the West Gondwanan margin.

The lowermost Selene Nunatak Formation crops out adjacent to the LeMay Group accretionary complex of central Alexander Island and forms a narrow band of ~150 m in thickness (Fig. 3). The Selene Nunatak Formation has an age profile that is akin to that of the adjacent LeMay Group 1 (Riley et al., 2023), with a prominent Late Permian peak and broad spread of Paleozoic ages. The close correlation between the LeMay Group 1 and Selene Nunatak Formation (unit 2) is evident in Figure 6, with both Selene Nunatak Formation samples plotting with a nearest neighbor relationship to LeMay Group 1, which indicates a likely source overlap. There is also a close clustering with samples from the Mount Peterson–Erewhon Beds of the southern Antarctic Peninsula and the Trinity Peninsula Group accretionary complex of the northern Antarctic Peninsula. The close clustering between the LeMay Group and the Mount Peterson–Erewhon Beds was investigated by Riley et al. (2023), who determined that although there is an overlap in age profiles, the Lu-Hf isotopic values are distinct, which suggests a different provenance. The close clustering with the Trinity Peninsula Group reflects a very similar provenance to the LeMay Group, as both units form part of a chain of Late Permian accretionary complexes.

The detrital zircon ages therefore strongly support direct recycling of units of LeMay Group 1 adjacent to the outcrop extent of the Selene Nunatak Formation and indicate a paleoflow from west to east. Although the age profiles of LeMay Group 1 and the Selene Nunatak Formation are overwhelmingly similar, a single younger age in the Selene Nunatak Formation before 200 Ma indicates a potentially younger age of deposition. Based on a weakly diagnostic belemnite assemblage, an approximate Early–Middle Jurassic age is also suggested by Doubleday et al. (1993), who also determined a sediment source from the arc in the east as well as the adjacent accretionary complex in the west.

There is an abrupt change in provenance between the Selene Nunatak Formation and the overlying Atoll Nunataks Formation, with a shift in source to the east (arc). The pebble sandstone from the Atoll Nunataks Formation has a prominent Early Jurassic age peak (ca. 183 Ma; Fig. 4C) that is akin to the Early Jurassic component of the Latady Group of southern Palmer Land. However, there is no close clustering between the Atoll Nunataks Formation (unit 3) and the Latady Group in the MDS plot (Fig. 6), which reflects the absence of a broad spectrum of older ages in the Atoll Nunataks Formation. However, the Lu-Hf isotopic data demonstrate a closer relationship (Fig. 5), where an overlap in εHf values between the Latady Group and the Atoll Nunataks Formation is evident. A likely maximum depositional age of ca. 177 Ma was determined (Fig. S2), which is somewhat older than the proposed Bajocian age (Butterworth et al., 1988).

No older U-Pb ages (post-220 Ma) were identified in the Atoll Nunataks Formation that would be anticipated if it were directly recycling components of the Latady Group, which is characterized by an array of early Paleozoic and Proterozoic ages (Riley et al., 2023). The volcanic input to the Latady Group was widely considered (e.g., Hunter and Cantrill, 2006) to be derived from the neighboring and essentially contemporaneous Mount Poster Formation (Pankhurst et al., 2000; Hunter et al., 2006). However, the εHf range of the Mount Poster Formation (ca. 183 Ma) is considerably more radiogenic (−13 to −8; Fig. 5A) than the Early Jurassic component of the Latady Group (−9 to −2; Fig. 5A). The implication is that the Early

Jurassic (ca. 183 Ma) components of both the Atoll Nunataks Formation and Latady Group were sourced from an episode of Early Jurassic magmatism other than the intraplate Mount Poster Formation (Riley et al., 2001). Early Jurassic arc magmatism is ubiquitous in the southern Antarctic Peninsula (e.g., Riley et al., 2017a; Velev et al., 2023) and the adjacent Thurston Island crustal block (Riley et al., 2017b). The adjacent Brennecke Formation of eastern Palmer Land (Fig. 1) is characterized by intermediate-silicic volcanic rocks that are distinct in composition from those of the Mount Poster Formation, which have a pronounced upper crustal component (Riley et al., 2001). The Brennecke Formation is less radiogenic and overlaps with the Early Jurassic volcanic rocks of Patagonia and Thurston Island (Riley et al., 2001, 2017b), although no Lu-Hf data are available. Given the absence of a broad spectrum of ages in the age profile of the Atoll Nunataks Formation (Fig. 4C), a proximal Early Jurassic volcanic source is favored, which is likely to be centered in western Palmer Land or potentially Thurston Island.

Interestingly, the Group 3 succession of the LeMay Group (Riley et al., 2023), which has a mid-Cretaceous depositional age (Charcot Island; Fig. 2), is also characterized by a prominent Early Jurassic age population with an εHf range of −12 to −7 (Fig. 5C), which overlaps with the age of the Mount Poster Formation.

The data indicate a significant hiatus (>_20 m.y.) prior to the deposition of the Ablation Point Formation, which forms an ~400-m-thick unit restricted to the eastern margin of Alexander Island and the western coast of northwest Palmer Land (Fig. 3). It has a likely maximum depositional age of ca. 155 Ma (Fig. S2), which is consistent with its Kimmeridgian molluscan fauna. The two samples from the Ablation Point Formation have Late Jurassic–dominated age profiles (ca. 157 and ca. 153 Ma), combined with a significant contribution from Middle Triassic zircon grains (Figs. 4D and 4E). An age peak of Late Jurassic ages in the Ablation Point Formation overlaps with age profiles from the upper parts of the Latady Group succession (ca. 152 Ma), with both units having similar depositional ages, and they may share a sediment source. A potential link to the upper Latady Group is also evident in Figure 6, with sample KG.3657.4 (unit 4) of the Ablation Point Formation having a nearest neighbor relationship to the Latady Group. However, with additional εHf data (Fig. 5A), the close relationship between the Ablation Point Formation and the upper Latady Group is not as robust; the εHf values (at ca. 150 Ma) for the upper Latady Group are typically <_0, compared to εHf values of >_2 (Fig. 5) for the Ablation Point Formation. These εHf values are amongst the highest across the Fossil Bluff Group and may have coincided with an episode of slab break-off during flat-slab subduction in the Antarctic Peninsula (Bastias et al., 2023).

There are no major magmatic sources for the Late Jurassic zircon population evident in the geological record of the Antarctic Peninsula, although minor volcanic units from Adelaide Island (Riley et al., 2012), Alexander Island (Macdonald et al., 1999), and Thurston Island (Riley et al., 2017b) have ages ranging from 155 Ma to 150 Ma. The Middle Triassic contribution to the age profile for the Ablation Point Formation is likely to be sourced from the adjacent granitoids of northwest Palmer Land, where Middle to Late Triassic magmatism and metamorphism (Fig. 1) has been widely recognized (Millar et al., 2002; Riley et al., 2020b; Bastias et al., 2023). The detrital zircon age profile for sample KG.3657.4 (Fig. 4E), from near Belemnite Point, has a mixed age population that indicates some degree of recycling of an eroded sediment source, but also a likely proximal Late Jurassic volcanic source.

Prior to deposition of the Himalia Ridge Formation, there is evidence of a Late Jurassic–Early Cretaceous episode of magmatic quiescence. A magmatic hiatus between ca. 153 Ma and 145 Ma is, to some extent, borne out in the detrital zircon data presented here (Fig. 7), with only limited evidence of magmatism in this interval. Bastias et al. (2023) also suggested a pause in magmatism during the interval 148–140 Ma but did not link the hiatus to any pause in subduction; instead, they favored a model involving increased obliquity during convergence. The Himalia Ridge Formation is an extensive unit, >2.5 km in thickness, and our data indicate

a likely depositional age of ca. 140 Ma (Fig. S2), which is consistent with a Tithonian–Berriasian age based on the molluscan fauna (Crame and Howlett, 1988). The succession was deposited as a series of migrating, conglomerate-filled inner-fan channels, with inner-channel mudstone and sandstone facies (Butterworth et al., 1988). The samples investigated here are from the mid- to upper part of the succession. The MDS analysis in Figure 6 indicates that these two samples (KG.3069.2 and KG.2883.4) have a nearest neighbor relationship to the upper part of the Latady Group (Nordsim Formation; Hunter and Cantrill, 2006), which also has a depositional age of ca. 140 Ma (Berriasian). The conglomerate beds in the upper part of the Himalia Ridge Formation are dominated by granitoid clasts instead of volcanic clasts, which Miller and Macdonald (2004) interpreted to represent unroofing of the magmatic arc to the east. The granitoid-only clasts from the Himalia Ridge Formation conglomerate (sample KG.3463.2) can be interpreted as the likely primary arc component of the Himalia Ridge Formation sandstones. The recycled component of the Himalia Ridge Formation sandstones is likely akin to the upper parts of the Latady Group. However, a direct source-to-sink relationship is not favored given the absence of Early Cambrian zircon grains that are ubiquitous in the Latady Group (Riley et al., 2023).

Two samples from the Early Cretaceous Spartan Glacier Formation have detrital zircon age profiles very similar to components of the Himalia Ridge Formation, but with marginally younger likely depositional ages (ca. 134 Ma; Fig. S2). The Spartan Glacier Formation has a dominant Early Cretaceous age peak that was likely sourced from the adjacent arc, but also a minor recycled component akin to elements of the upper Latady Group, with characteristic Early Jurassic (ca. 184 Ma) and mid-Triassic (ca. 218 Ma) age peaks (Figs. 4I and 4J).
The Pluto Glacier Formation forms the most extensive unit of the southern and central Fossil Bluff Group. Three samples from across a broad section of the Pluto Glacier Formation all exhibit very similar detrital zircon age profiles (Figs. 4K–4M). All exhibit a strong primary magmatic arc signature with little input from recycled sources. The εHf values (Fig. 5A) of the Pluto Glacier Formation closely overlap with the suite of Early Cretaceous granitoids of Palmer Land (Bastias et al., 2023) and support the direct input of a proximal arc source into the shallowing forearc basin. The uppermost Neptune Glacier Formation is almost 3 km in thickness, and two samples from the lower and central part of the succession are examined here. Sample J6.288.2 is from Adelaide Island and forms a northern extension of the forearc succession; it is interpreted to form an equivalent unit to the Deimos Ridge Member (unit 8) of Alexander Island. Sample J6.288.2 has a primary age peak of ca. 115 Ma (two distinct peaks at ca. 112 and ca. 118 Ma; Fig. 4N) and a second Early Cretaceous peak at ca. 134 Ma. Sample KG.4956.1, from the Triton Point Member (unit 9), has a marginally younger age profile, which is characterized by two mid-Cretaceous age peaks at ca. 105 Ma and ca. 124 Ma (Fig. 4O). Both samples are dominated by locally sourced input from the adjacent arc with almost no recycling of any early Mesozoic or Paleozoic material. However, there is a significant degree of recycling of mid- to Early Cretaceous material involved in the deposition of the upper parts of the Fossil Bluff Group. Hf data are only available from the uppermost sample from Coal Nunatak (KG.4956.1), which overlaps with the adjacent mid-Cretaceous arc magmatism from northwest Palmer Land (Riley et al., 2020a; Bastias et al., 2023) and the extensive, but more distal, Lassiter Coast intrusive suite of eastern Palmer Land (Riley et al., 2018). Samples from the Neptune Glacier Formation have no nearest neighbor relationship or clustering in MDS analysis with any of the pre-Cretaceous sedimentary succession, which indicates that their age profiles are dominated by a proximal arc magmatic input.

## 6. DISCUSSION

The late Mesozoic is one of the most dynamic periods of convergent margin magmatism and tectonic activity across the Antarctic Peninsula and elsewhere in West Antarctica. However, the late Mesozoic magmatic arc record is unlikely to be complete because the volcanic units have been eroded, and their intrusive counterparts are unevenly distributed. Also, the direct data record is compromised because access to large sections of the Antarctic Peninsula is not possible due to its terrain and ice cover. Therefore, it is not possible to construct an

uninterrupted record of the pulses and pauses in arc magmatism. The detrital zircon age and εHf record of a long-lived late Mesozoic forearc basin in Alexander Island has the potential to complement the magmatic record and provide a more complete history of magmatism and subduction dynamics in a continental margin arc setting where zircon is frequently a component of the magmatic rocks. The forearc basin of Alexander Island records a largely complete record of sedimentation through the late Mesozoic and is dominated by litho-feldspathic sandstones, mudstones, conglomerate beds, and rare volcanic horizons, with paleocurrent evidence indicating a dominant source to the east from the magmatic arc (Butterworth et al., 1988).

Schwartz et al. (2021) suggested the primary sedimentary source for a Cordilleran magmatic forearc basin would be derived from the volcanic carapace and erosion of the uplifted granitoid plutonic belt, and Cawood et al. (2012) demonstrated that forearc settings are dominated by sediment sourced from the proximal arc. Condie et al. (2009) and Schwartz et al. (2021) highlighted that igneous age peaks do not always have detrital counterparts and vice versa, which lends support for examining both the magmatic and detrital record to interpret the tempo of the arc (Surpless et al., 2019). Our analysis of the Fossil Bluff Group, combined with existing analysis of the Mesozoic magmatic record, now permits a fuller examination of the coupled arc-basin system.

More than 1000 new zircon (U-Pb) analyses are presented, along with 560 zircon (Lu-Hf) analyses, from a suite of 15 samples from across the entire Fossil Bluff Group. Combined U-Pb and Lu-Hf analysis in zircon has been used previously (e.g., Nelson and Cottle, 2018) to infer periods of accelerated extension and contraction at convergent margins. The detrital zircon record is dominated by Cretaceous (n = 589) grains sourced from the proximal magmatic arc, with a varying supply of primary and recycled Jurassic grains, as well as recycled Triassic and Paleozoic zircon grains, particularly in the lower parts of the Fossil Bluff Group. Significant zircon age peaks have been identified at ca. 105 Ma, 125–131 Ma, 141 Ma, 154 Ma, and 183 Ma (Fig. 7), with notable pauses in magmatism between ca. 120–108 Ma, ca. 152–145 Ma, and ca. 177–ca. 160 Ma (Fig. 7). The mid-Cretaceous magmatic events at ca. 105 Ma, 115 Ma, and 125 Ma are well recognized from the southern Antarctic Peninsula, particularly eastern Palmer Land (Lassiter Coast intrusive suite; Riley et al., 2018) and to some extent, central Palmer Land (Flowerdew et al., 2005; Riley et al., 2020a; Bastias et al., 2023). The Early Cretaceous events (ca. 130 Ma and 141 Ma; Fig. 7) are the most significant across the Fossil Bluff Group but are not as ubiquitous in the magmatic record of the Antarctic Peninsula, although Bastias et al. (2023) recognized components of Early Cretaceous magmatism across western Palmer Land, and also central Graham Land. The Late Jurassic age peak at ca. 154 Ma is a prominent feature of the Kimmeridgian Ablation Point Formation and is also a major component of the Latady Group sedimentary rocks of southern Palmer Land (Riley et al., 2023). Magmatism at ca. 155 Ma was recognized by Pankhurst et al. (2000) as representing a significant magmatic pulse (V event; 157–153 Ma) across southern Patagonia (Chon Aike Province) but was essentially absent in the magmatic record of the Antarctic Peninsula. However, the detrital zircon record of the Latady Group and the Ablation Point Formation indicates that the V3 event of Patagonia, although largely absent in the volcanic-plutonic record, is well-preserved in the detrital record of the forearc and retro/back-arc setting (Latady Group).

The Early Jurassic age peak at ca. 183 Ma is prominent in the Atoll Nunataks Formation, forming ~90% of the detrital zircon population, but is also widespread as a secondary age population throughout the Fossil Bluff Group. The Atoll Nunataks Formation has an Early Jurassic (ca. 177 Ma) likely maximum depositional age (Fig. S2), and the Early Jurassic age peak is derived from a proximal arc, and not a recycled source, based on its detrital zircon age profile (Fig. 4C). The source for the Early Jurassic age population is distinct from the widespread Mount Poster Formation of southern Palmer Land, which is characterized by strongly radiogenic εHf values, whereas the ca. 183 Ma population recorded in the Atoll Nunataks Formation and as subsidiary peaks across the lower part of the Fossil Bluff Group succession has much less radiogenic values (Fig. 5A) and overlaps with parts of the Latady Group (Fig. 5B; Riley et al., 2023). The implication is that an Early Jurassic volcanic source, isotopically distinct from the Mount Poster Formation, which is not preserved in the magmatic record, was present during deposition of the Atoll Nunataks Formation and parts of the Latady Group. The Mount Poster Formation is a suite of rhyodacitic ignimbrites that were strongly controlled by upper crustal processes (Riley et al., 2001) and were emplaced in the interval 185–181 Ma (Hunter et al., 2006), likely in an intraplate setting. The εHf values of ca. 183 Ma zircons from across the Fossil Bluff Group (Fig. 5A), and components of the Latady Group (Fig. 5B), indicate a separate phase of volcanism with a more minor upper crustal component, potentially akin to the Early Jurassic arc magmatism of the Antarctic Peninsula (Riley et al., 2017a). This episode may be a marginally later phase of volcanism associated with the Mount Poster Formation, but with shorter residence times in the upper crust. Interestingly, the mid-Cretaceous sedimentary succession at Charcot Island off the coast of western Alexander Island (Fig. 2) also has a significant Early Jurassic detrital zircon component that overlaps closely with the εHf values (Fig. 5C) of the Mount Poster Formation (Riley et al., 2023) and indicates a shift in source-to-sink dynamics during the late Mesozoic. This is also evident from a single Early Jurassic detrital zircon from the mid-Cretaceous Pluto Glacier Formation, which has an εHf value (~−8; Fig. 5A) that also overlaps with the Mount Poster Formation.

The depositional environment for the Atoll Nunataks Formation was considered by Holdsworth and Nell (1992) as a trench-slope setting, as opposed to a forearc basin setting. Given the Early Jurassic depositional age of the lowermost units of the Fossil Bluff Group and a likely 20 m.y. hiatus before the deposition of the Ablation Point Formation, it is likely that the depositional environment of the lowermost sequences of the Fossil Bluff Group is distinct to the main forearc succession, which did not develop until the Late Jurassic. The hiatus between ca. 177 Ma and ca. 155 Ma (Fig. 7), prior to the development of the main phase of forearc deposition, reflects the near absence of magmatism in Palmer Land during the Middle Jurassic, with the main locus of magmatism developing across the northern Antarctic Peninsula. The Mapple Formation (and its correlatives) of northern and eastern Graham Land (Fig. 1) were emplaced in the interval 175–163 Ma (Riley and Leat, 1999; Pankhurst et al., 2000; Riley et al., 2010; Riley and Leat, 2021) and formed part of the V2 event of the widespread Chon Aike Province (Pankhurst et al., 1998).

Evidence of another significant hiatus in Late Jurassic magmatism in the Antarctic Peninsula has been tentatively suggested by several authors (e.g., Leat et al., 1995; Bastias et al., 2021) but was often based on an incomplete geochronological record from isolated outcrops. The detrital zircon record of the Fossil Bluff Group suggests there may be a minor pause in the magmatic record between ca. 153 Ma and 145 Ma. This pause in magmatism is also identified across Graham Land (Bastias et al., 2021) and Patagonia (Pankhurst et al., 2000) and may correlate with changes in slab dynamics (Nelson and Cottle, 2018), as opposed to any pause in subduction (Bastias et al., 2021). However, a significant pause in continental margin arc magmatism is predicted in some models (e.g., Riley et al., 2001) following magmatic “flare up” events. Throughout the Jurassic, the West Gondwanan margin was punctuated by several high-flux magmatic events dominated by silicic volcanism and granitoid emplacement (Chon

Aike Province; Pankhurst et al., 1998). High levels of silicic-intermediate magmatism over prolonged periods will deplete the most fusible parts of the crust and inevitably lead to a pause in eruptible magmatism (Bryan et al., 2002). Therefore, the hiatus in magmatism following the emplacement of the Chon Aike Province (188–153 Ma; Pankhurst et al., 2000) may be a consequence of changes in crustal processes, rather than any slab dynamic processes.

The source-to-sink mechanics of the Fossil Bluff Group are strongly controlled by the supply of sediment from local magmatic sources (cf. Cawood et al., 2012). The absence of any significant population of Middle Jurassic zircon grains (175–160 Ma) in the Fossil Bluff Group is strongly suggestive of a strong Palmer Land bias as the primary source into the forearc basin (Fig. 8). Middle Jurassic volcanic and plutonic rocks are widespread in northern and eastern Graham Land, and form an extension of the V2 event of the Chon Aike Province (Pankhurst et al., 2000). By contrast, Middle Jurassic magmatism in Palmer Land is essentially absent, and therefore, a strong Palmer Land source bias for the Fossil Bluff Group is supported. Also, the ubiquitous occurrence of Late Triassic and Early Jurassic age populations in the Fossil Bluff Group strongly indicates a Palmer Land source bias, as both age populations are rare in the northern sector of the Antarctic Peninsula. Potential sediment sources farther south (e.g., Marie Byrd Land; Fig. 1) are also unlikely; the εHf isotopic envelope (Fig. 5A) for Marie Byrd Land (Nelson and Cottle, 2018) lies significantly outside the range of the Fossil Bluff Group units, particularly for Triassic–Jurassic components.
The uppermost succession exposed in the basin was deposited at ca. 103 Ma (Mars Glacier Member; Moncrieff and Kelly, 1993; Fig. 7) and reflects the large-scale shallowing in the forearc basin. Its deposition was coincident with phase 2 of the Palmer Land tectonic event, an episode of dextral transpression (Vaughan et al., 2012). The event is also associated with the development of unconformities in northwest Palmer Land (Leat et al., 2009), and the compressional event marks the transition to an eventual transtensional regime in the Late Cretaceous (Vaughan et al., 2012). If the Mars Glacier Member represents the cessation of deposition into the forearc basin, it may also overlap with the development of oroclinal bending of the Antarctic Peninsula and Patagonia as a consequence of plate vector changes (Poblete et al., 2016). The Fossil Bluff Group forearc basin underwent exhumation at ca. 100 Ma (Storey et al., 1996), and the underlying LeMay Group accretionary complex also exhibits evidence of compressive deformation associated with this event.

Several authors have considered an allochthonous origin for Alexander Island (Vaughan and Storey, 2000; Burton-Johnson and Riley, 2015; Bastias et al., 2023), with terrane translation and “docking” with the Eastern Domain (Fig. 1) of the Antarctic Peninsula occurring during the mid-Cretaceous as part of the Palmer Land Event at ca. 103 Ma (Vaughan et al., 2012). This model implies that the deposition of the entire Fossil Bluff Group developed prior to terrane

translation and docking. The provenance signal of the Fossil Bluff Group presented here indicates a strong local bias, with direct recycling of arc material from western Palmer Land during the Cretaceous and a ubiquitous Middle Triassic signal that is also consistent with a likely source from northwest Palmer Land. This age profile could be consistent with the Western Domain forming part of a subduction-accretionary complex with the Central Domain (Vaughan and Storey, 2000). However, the episode of magmatism at ca. 155 Ma that is present in the detrital record of parts of the Fossil Bluff Group (Ablation Point Formation) and also the Latady Group succession of the Eastern Domain indicates a likely proximal relationship between the Western and Eastern domains during the Late Jurassic. Therefore, an autochthonous model for Alexander Island throughout the Jurassic to the mid-Cretaceous is preferred.

The depositional environment and the locus of arc magmatism can have a significant influence on the detrital zircon profile of the sedimentary succession, influencing the variable input of primary and recycled material. The lowermost sequence (Selene Nunatak Formation) is almost entirely composed of recycled material from the adjacent Late Permian accretionary complex (to the west), whereas the overlying Atoll Nunataks Formation is sourced from a proximal Early Jurassic magmatic event into a trench-slope environment (to the east). Following an ~20 m.y. hiatus, the renewed onset of sedimentation into the forearc basin at ca. 157–153 Ma is dominated by a strongly recycled signature, with Middle Triassic and Paleozoic sources forming a significant component of the Ablation Point and Himalia Ridge formations. Following a brief (~10 m.y.) Late Jurassic hiatus in sedimentation, the Spartan Glacier Formation is also characterized by a mixed arc/recycled signature. But during the Early–mid-Cretaceous, the Fossil Bluff Group is dominated by a primary arc signature from a presumed proximal source in western Palmer Land. This latter phase of deposition into the shallowing forearc basin was significant, with ~4 km of sedimentation preserving a relatively complete arc magmatic record.

## 7. CONCLUSIONS

(1) Deposition in a trench slope environment initiated in the Early Jurassic at ca. 180 Ma. The basal unit of the Fossil Bluff Group (Selene Nunatak Formation) is locally derived from the adjacent Late Permian accretionary complex (LeMay Group), with potentially minor input from the magmatic arc.
(2) The Early Jurassic signature of the lower Fossil Bluff Group (Atoll Nunataks Formation) is directly derived from a proximal Early Jurassic magmatic source. This source is distinct from the widespread Mount Poster Formation of southern Palmer Land and indicates a separate phase of Early Jurassic (possibly arc) magmatism that is no longer present in the geological record.
(3) In Palmer Land, there was a likely hiatus in magmatism and deposition of ~20 m.y. during the Middle Jurassic prior to the onset of forearc sedimentation during the Late Jurassic.
(4) The V3 event of the widespread Chon Aike Province, which has no significant magmatic record in the Antarctic Peninsula, is well preserved in the Late Jurassic sedimentary record of the Fossil Bluff Group and also the upper Latady Group of eastern Palmer Land.
(5) The main phase of forearc deposition developed during the Late Jurassic–mid Cretaceous, with an ~6-km-thick sequence directly derived from the late Mesozoic magmatic arc into a shallowing forearc basin (Fig. 8). The episode of Early Cretaceous magmatism (ca. 140 Ma), which is dominant in the detrital record of the Fossil Bluff Group, is poorly preserved in the magmatic record.
(6) Forearc basin deposition is strongly controlled by the proximal arc in western Palmer Land and is characterized by a mixed arc/recycled signature during episodes of renewed sedimentation. However, deposition during the Early Jurassic (ca. 180 Ma) and Early Cretaceous (141–131 Ma) was dominated by arc-only sources.
(7) εHf (zircon) records potential tectonic shifts from convergence (Early Jurassic) to extension (Late Jurassic–Early Cretaceous), prior to a strong trend to renewed convergence during the mid-Cretaceous. This reflects the trend identified along large sectors of accretionary orogens of the West Gondwanan margin (Nelson and Cottle, 2018). This trend is clearly defined in the detrital

zircon record of the Fossil Bluff Group, where previously the direct magmatic record was incomplete.
(8) The zircon (U-Pb and Lu-Hf) data support an autochthonous origin for the Western and Central domains and a common provenance with the Eastern Domain of the Antarctic Peninsula during the Late Jurassic.

**REFERENCES CITED**


Barbeau, D.L., Davis, J.T., Murray, K.E., Valencia, V., Gehrels, G.E., Zahid, K.M., and Gombosi, D.J., 2010, Detrital-zircon geochronology of the metasedimentary rocks of north-western Graham Land: Antarctic Science, v. 22, p. 65–78, https://doi .org /10 .1017 /S095410200999054X.

Bastias, J., Spikings, R., Riley, T., Ulianov, A., Grunow, A., Chiaradia, M., and Hervé, F., 2021, A revised interpretation of the Chon Aike magmatic province: Active margin origin and implications for the opening of the Weddell Sea: Lithos, v. 386–387, https://doi .org /10 .1016 /j .lithos .2021 .106013.

Bastias, J., Spikings, R., Riley, T., Chew, D., Grunow, A., Ulianov, A., Chiaradia, M., and Burton-Johnson, A., 2023, Cretaceous magmatism in the Antarctic Peninsula and its tectonic implications: Journal of the Geological Society, v. 180, https://doi .org /10 .1144 /jgs2022-067.

Bouvier, A., Vervoort, J.D., and Patchett, P.J., 2008, The Lu–Hf and Sm–Nd isotopic composition of CHUR: Constraints from unequilibrated chondrites and implications for the bulk composition of terrestrial planets: Earth and Planetary Science Letters, v. 273, p. 48–57, https://doi .org /10 .1016 /j .epsl .2008 .06 .010.

Bryan, S.E., Riley, T.R., Jerram, D.A., Stephens, C.J., and Leat, P.T., 2002, Silicic volcanism: An undervalued component of large igneous provinces and volcanic rifted margins, *in* Menzies, M.A., Klemperer, S.L., Ebinger, C.J., and Baker, J.A., eds., Volcanic Rifted Margins: Geological Society of America Special Paper 362, p. 97–118, https://doi .org /10 .1130 /0-8137 -2362-0 .97.

Burton-Johnson, A., and Riley, T.R., 2015, Autochthonous vs. accreted terrane development of continental margins: A new in situ tectonic history of the Antarctic Peninsula: Journal of the Geological Society, v. 172, p. 822–835, https://doi .org /10 .1144 /jgs2014-110.

Burton-Johnson, A., Riley, T.R., Harrison, R.J., MacNiocaill, C., Muraszko, J.R., and Rowley, P.D., 2022, Granitic magnetic fabrics show tectonic deformation control of episodic continental arc magmatism: Gondwana Research, v. 112, https://doi .org /10 .1016 /j .gr .2022 .09 .006.

Butterworth, P.J., 1991, The role of eustasy in the development of a regional shallowing event in a tectonically active basin, Fossil Bluff Group Jurassic–Cretaceous, Alexander Island, Antarctica, *in* Macdonald, D.I.M., ed., Sedimentation, Tectonics and Eustasy: Sea Level Changes at Active Margins: International Association of Sedimentologists Special Publication 12, p. 307–329, https://doi .org /10 .1002 /9781444303896 .ch18.

Butterworth, P.J., Crame, J.A., Howlett, P.J., and Macdonald, D.I.M., 1988, Lithostratigraphy of Upper Jurassic–Lower Cretaceous strata of eastern Alexander Island: Cretaceous Research, v. 9, p. 249–264, https://doi .org /10 .1016 /0195-6671(88)90020-1.

Castillo, P., Lacassie, J.P., Augustsson, C., and Hervé, F., 2015, Petrography and geochemistry of the Carboniferous–Triassic Trinity Peninsula Group, West Antarctica: Implications for provenance and tectonic setting: Geological Magazine, v. 152, p. 575–588, https://doi .org /10 .1017 /S0016756814000454.

Castillo, P., Fanning, C.M., Hervé, F., and Lacassie, J.P., 2016, Characterisation and tracing of Permian magmatism in the south-western segment of the Gondwana margin: U-Pb age, Lu-Hf and O isotopic compositions of detrital zircons from metasedimentary complexes of northern Antarctic Peninsula and western Patagonia: Gondwana Research, v. 36, p. 1–13, https://doi .org /10 .1016 /j .gr .2015 .07 .014.

Cawood, P.A., Hawkesworth, C.J., and Dhuime, B., 2012, Detrital zircon record and tectonic setting: Geology, v. 40, p. 875–878, https://doi .org /10 .1130 /G32945 .1.

Condie, K.C., Belousova, E., Griffin, W.L., and Sircombe, K.N., 2009, Granitoid events in space and time: Constraints from igneous and detrital zircon age spectra: Gondwana Research, v. 15, p. 228–242, https://doi .org /10 .1016 /j .gr .2008 .06 .001.

Crame, J.A., and Francis, J.E., 2024, Cretaceous stratigraphy of Antarctica and its global significance, *in* Hart, M.B., Batenburg, S.J., Huber, B.T., Prince, G.D., Thibault, N., Wagreich, M., and Walaszczyk, I., eds., Cretaceous Project 200 Volume 2: Regional Studies: Geological Society, London, Special Publication 545, https://doi .org /10 .1144 /SP545-2023-153.
Crame, J.A., and Howlett, P.J., 1988, Late Jurassic and Early Cretaceous biostratigraphy of the Fossil Bluff Formation, Alexander Island: British Antarctic Survey Bulletin, v. 78, p. 1–35.
Dobbs, S.C., Malkowski, M.A., Schwartz, T.M., Sickmann, Z.T., and Graham, S.A., 2022, Depositional controls on detrital zircon provenance: An example from Upper Cretaceous strata, southern Patagonia: Frontiers of Earth Science, v. 10, https://doi .org /10 .3389 /feart .2022 .824930.
Doubleday, P.A., and Storey, B.C., 1998, Deformation history of a Mesozoic forearc basin sequence on Alexander Island, Antarctic Peninsula: Journal of South American Earth Sciences, v. 11, p. 1–21, https://doi .org /10 .1016 /S0895-9811(97)00032-1.
Doubleday, P.A., Macdonald, D.I.M., and Nell, P.A.R., 1993, Sedimentology and structure of the trench-slope to fore-arc basin transition in the Mesozoic of Alexander Island, Antarctica: Geological Magazine, v. 130, p. 737–754, https://doi .org /10 .1017 /S0016756800023128.
Edwards, C.W., 1979, New evidence of major faulting on Alexander Island: British Antarctic Survey Bulletin, v. 49, p. 15–20.
Elliot, D.H., Fanning, C.M., and Laudon, T.S., 2016, The Gondwana Plate margin in the Weddell Sea sector: Zircon geochronology of Upper Palaeozoic mainly Permian strata from the Ellsworth Mountains and eastern Ellsworth Land, Antarctica: Gondwana Research, v. 29, p. 234–247, https://doi .org /10 .1016 /j .gr .2014 .12 .001.
Farquharson, G.W., 1984, Late Mesozoic, non-marine conglomeratic sequences of northern Antarctic Peninsula (The Botany Bay Group): British Antarctic Survey Bulletin, v. 65, p. 1–32.
Flowerdew, M.J., Millar, I.L., Vaughan, A.P.M., and Pankhurst, R.J., 2005, Age and tectonic significance of the Lassiter Coast Intrusive Suite, eastern Ellsworth Land, Antarctic Peninsula: Antarctic Science, v. 17, p. 443–452, https://doi .org /10 .1017 /S09541 02005002877.
Gao, L., Pei, J.L., Zhao, Y., Yang, Z.Y., Riley, T.R., Liu, X.C., Zhang, S.H., and Liu, J.M., 2021, New paleomagnetic constraints on the Cretaceous tectonic framework of the Antarctic Peninsula: Journal of Geophysical Research: Solid Earth, v. 126, https://doi .org /10 .1029 /2021JB022503.
Guenthner, W.R., Barbeau, D.L., Jr., Reiners, P.W., and Thomson, S.N., 2010, Slab window migration and terrane accretion preserved by low-temperature thermochronology of a magmatic arc, northern Antarctic Peninsula: Geochemistry, Geophysics, Geosystems, v. 11, https://doi .org /10 .1029 /2009GC002765.
Holdsworth, B.K., and Nell, P.A.R., 1992, Mesozoic radiolarian faunas from the Antarctic Peninsula: Age, tectonic and palaeoceanographic significance: Journal of the Geological Society, v. 149, p. 1003–1020, https://doi .org /10 .1144 /gsjgs .149 .6.1003.
Hunter, M.A., and Cantrill, D.J., 2006, A new stratigraphy for the Latady Basin, Antarctic Peninsula: Part 2, Latady Group and basin evolution: Geological Magazine, v. 143, p. 797–819, https://doi .org /10 .1017 /S00167 56806002603.
Hunter, M.A., Cantrill, D.J., Flowerdew, M.J., and Millar, I.L., 2005, Mid-Jurassic age for the Botany Bay Group: Implications for Weddell Sea Basin creation and southern hemisphere biostratigraphy: Journal of the Geological Society, v. 162, p. 745–748, https://doi .org /10 .1144 /0016-764905-051.
Hunter, M.A., Riley, T.R., Cantrill, D.J., Flowerdew, M.J., and Millar, I.L., 2006, A new stratigraphy for the Latady Basin, Antarctic Peninsula: Part 1, Ellsworth Land volcanic group: Geological Magazine, v. 143, p. 777–796, https://doi .org /10 .1017 /S0016756806002597.
Hyden, G., and Tanner, P.W.G., 1981, Late-Palaeozoic–early Mesozoic fore-arc basin sedimentary rocks at
 

the Pacific margin in Western Antarctica: Geologische Rundschau, v. 70, p. 529–541, https://doi .org /10 .1007 /BF01822133.
Jarrard, R.D., 1986, Terrane motion by strike-slip faulting of forearc slivers: Geology, v. 14, p. 780–783, https://doi .org /10 .1130 /0091-7613(1986)14<_780:TMBSFO>_2 .0.CO;2.
Jeon, H., and Whitehouse, M.J., 2015, A critical evaluation of U–Pb calibration schemes used in SIMS zircon geochronology: Geostandards and Geoanalytical Research, v. 39, p. 443–452, https://doi .org /10 .1111 /j .1751-908X .2014 .00325 .x.
Jordan, T.A., Neale, R.F., Leat, P.T., Vaughan, A.P.M., Flowerdew, M.J., Riley, T.R., Whitehouse, M.J., and Ferraccioli, F., 2014, Structure and evolution of Cenozoic arc magmatism on the Antarctic Peninsula; a high resolution aeromagnetic perspective: Geophysical Journal International, v. 198, p. 1758–1774, https://doi .org /10 .1093 /gji /ggu233.
Larter, R.D., and Barker, P.F., 1991, Effects of ridge crest–trench interaction on Antarctic–Phoenix spreading: Forces on a young subducting plate: Journal of Geophysical Research: Solid Earth, v. 96, p. 19,583–19,607, https://doi .org /10 .1029 /91JB02053.
Leat, P.T., Scarrow, J.H., and Millar, I.L., 1995, On the Antarctic Peninsula batholith: Geological Magazine, v. 132, p. 399–412, https://doi .org /10 .1017 /S0016756800021464.
Leat, P.T., Flowerdew, M.J., Riley, T.R., Whitehouse, M.J., Scarrow, J.H., and Millar, I.L., 2009, Zircon U-Pb dating of Mesozoic volcanic and tectonic events in north-west Palmer Land and south-west Graham Land, Antarctica: Antarctic Science, v. 21, p. 633–641, https://doi .org /10 .1017 /S0954102009990320.
Macdonald, D.I.M., and Butterworth, P.J., 1986, Slope collapse deposits in a Mesozoic marine fore-arc basin, Antarctica: International Sedimentological Congress, 12th, Canberra, Australia, Abstracts, p. 193–194.
Macdonald, D.I.M., Leat, P.T., Doubleday, P.A., and Kelly, S.R.A., 1999, On the origin of fore-arc basins: New evidence of formation by rifting from the Jurassic of Alexander Island, Antarctica: Terra Nova, v. 11, p. 186–193, https://doi .org /10 .1046 /j .1365-3121 .1999 .00244 .x.
Matthews, K.J., Seton, M., and Müller, R.D., 2012, A global-scale plate reorganization event at 105–100 Ma: Earth and Planetary Science Letters, v. 355–356, p. 283–298, https://doi .org /10 .1016 /j .epsl .2012 .08 .023.
McCarron, J.J., and Millar, I.L., 1997, The age and stratigraphy of fore-arc magmatism on Alexander Island, Antarctica: Geological Magazine, v. 134, no. 4, p. 507–522, https://doi .org /10 .1017 /S0016756897007437.
Milan, L.A., Daczko, N.R., and Clarke, G.L., 2017, Cordillera Zealandia: A Mesozoic arc flare-up on the palaeo-Pacific Gondwana margin: Scientific Reports, v. 7, p. 261, https://doi .org /10 .1038 /s41598-017-00347-w.
Millar, I.L., Pankhurst, R.J., and Fanning, C.M., 2002, Basement chronology and the Antarctic Peninsula: Recurrent magmatism and anatexis in the Palaeozoic Gondwana Margin: Journal of the Geological Society, v. 159, p. 145–157, https://doi .org /10 .1144 /0016 -764901-020.
Miller, S., and Macdonald, D.I.M., 2004, Metamorphic and thermal history of a fore-arc basin: The Fossil Bluff Group, Alexander Island, Antarctica: Journal of Petrology, v. 45, no. 7, p. 1453–1465, https://doi .org /10 .1093 /petrology /egh025.
Moncrieff, A.C.M., and Kelly, S.R.A., 1993, Lithostratigraphy of the uppermost Fossil Bluff Group Early Cretaceous of Alexander Island, Antarctica: History of an Albian regression: Cretaceous Research, v. 14, p. 1–15, https://doi .org /10 .1006 /cres .1993 .1001.
Nell, P.A.R., and Storey, B.C., 1991, Strike-slip tectonics within the Antarctic Peninsula fore-arc, *in* Thomson, M.R.A., Crame, J.A., and Thomson, J.W., eds., Geological Evolution of Antarctica: Cambridge, UK, Cambridge University Press, p. 443–448.
Nelson, D.A., and Cottle, J.M., 2018, The secular development of accretionary orogens: Linking the Gondwana magmatic arc record of West Antarctica, Australia and South America: Gondwana Research, v. 63, p. 15–33, https://doi .org /10 .1016 /j .gr .2018 .06 .002.
Nichols, G.J., and Cantrill, D.J., 2002, Tectonic and climatic controls on a Mesozoic forearc basin succession, Alexander Island, Antarctica: Geological Magazine, v. 139, p. 313–330, https://doi .org /10 .1017 /S0016 756802006465.

Noda, A., 2016, Forearc basins: Types, geometries, and relationships to subduction zone dynamics: Geological Society of America Bulletin, v. 128, p. 879–895, https://doi .org /10 .1130 /B31345 .1.
Pankhurst, R.J., Leat, P.T., Sruoga, P., Rapela, C.W., Marquez, M., Storey, B.C., and Riley, T.R., 1998, The Chon-Aike silicic igneous province of Patagonia and related rocks in Antarctica: A ailicic LIP: Journal of Volcanology and Geothermal Research, v. 81, p. 113–136, https://doi .org /10 .1016 /S0377-0273(97)00070-X.
Pankhurst, R.J., Weaver, S.D., Hervé, F., and Larrondo, P., 1999, Mesozoic–Cenozoic evolution of the North Patagonian batholith in Aysén, southern Chile: Journal of the Geological Society, v. 156, p. 673–694, https://doi .org /10 .1144 /gsjgs .156 .4.0673.
Pankhurst, R.J., Riley, T.R., Fanning, C.M., and Kelley, S.P., 2000, Episodic silicic volcanism in Patagonia and the Antarctic Peninsula: Chronology of magmatism associated with break-up of Gondwana: Journal of Petrology, v. 41, p. 605–625, https://doi .org /10 .1093 /petrology /41 .5.605.
Poblete, F., Roperch, P., Arriagada, C., Ruffet, G., de Arellano, C.R., Hervé, F., and Poujol, M., 2016, Late Cretaceous–early Eocene counterclockwise rotation of the Fueguian Andes and evolution of the Patagonia-Antarctic Peninsula system: Tectonophysics, v. 668–669, p. 15–34, https://doi .org /10 .1016 /j .tecto .2015 .11 .025.
Riley, T.R., and Leat, P.T., 1999, Large volume silicic volcanism along the proto-Pacific margin of Gondwana: Lithological and stratigraphical investigations from the Antarctic Peninsula: Geological Magazine, v. 136, p. 1–16, https://doi .org /10 .1017 /S0016756899002265.
Riley, T.R., and Leat, P.T., 2021, Palmer Land and Graham Land volcanic groups (Antarctic Peninsula): Volcanology, *in* Smellie, J.L., Panter, K.S., and Geyer, A., eds., Volcanism in Antarctica: 200 Million Years of Subduction, Rifting and Continental Break-up: Geological Society, London, Memoir 55, p. 121–138, https://doi .org /10 .1144 /M55-2018-36.
Riley, T.R., Leat, P.T., Pankhurst, R.J., and Harris, C., 2001, Origins of large volume silicic volcanism in the Antarctic Peninsula and Patagonia by crustal melting: Journal of Petrology, v. 42, p. 1043–1065, https://doi .org /10 .1093 /petrology /42 .6.1043.
Riley, T.R., Flowerdew, M.J., Hunter, M.A., and Whitehouse, M.J., 2010, Middle Jurassic rhyolite volcanism of eastern Graham Land, Antarctic Peninsula: Age correlations and stratigraphic relationships: Geological Magazine, v. 147, p. 581–595, https://doi .org /10 .1017 /S0016756809990720.
Riley, T.R., Flowerdew, M.J., and Whitehouse, M.J., 2012, Litho- and chronostratigraphy of a fore- to intra-arc basin: Adelaide Island, Antarctic Peninsula: Geological Magazine, v. 149, p. 768–782, https://doi .org /10 .1017 /S0016756811001002.
Riley, T.R., Flowerdew, M.J., Pankhurst, R.J., Curtis, M.L., Millar, I.L., Fanning, C.M., and Whitehouse, M.J., 2017a, Early Jurassic subduction-related magmatism on the Antarctic Peninsula and potential correlation with the Subcordilleran plutonic belt of Patagonia: Journal of the Geological Society, v. 174, p. 365–376, https://doi .org /10 .1144 /jgs2016-053.
Riley, T.R., Flowerdew, M.J., Pankhurst, R.J., Leat, P.T., Millar, I.L., Fanning, C.M., and Whitehouse, M.J., 2017b, A revised geochronology of Thurston Island, West Antarctica and correlations along the proto-Pacific margin of Gondwana: Antarctic Science, v. 29, p. 47–60, https://doi .org /10 .1017 /S0954102016000341.
Riley, T.R., Burton-Johnson, A., Flowerdew, M.J., and Whitehouse, M.J., 2018, Episodicity within a mid-Cretaceous magmatic flare-up in West Antarctica: U-Pb ages of the Lassiter Coast intrusive suite, Antarctic Peninsula and correlations along the Gondwana margin: Geological Society of America Bulletin, v. 130, p. 1177–1196, https://doi .org /10 .1130 /B31800 .1.
Riley, T.R., Flowerdew, M.J., Burton-Johnson, A., Leat, P.T., Millar, I.L., and Whitehouse, M.J., 2020a, Cretaceous arc volcanism of Palmer Land, Antarctic Peninsula: Zircon U-Pb geochronology, geochemistry, distribution and field relationships: Journal of Volcanology and Geothermal Research, v. 401, https://doi .org /10 .1016 /j .jvolgeores .2020 .106969.
Riley, T.R., Flowerdew, M.J., Millar, I.L., and Whitehouse, M.J., 2020b, Triassic magmatism and metamorphism in the Antarctic Peninsula: Identifying the extent and timing of the Gondwanide

Orogeny: Journal of South American Earth Sciences, v. 103, https://doi .org /10 .1016 /j .jsames .2020 .102732.
Riley, T.R., Millar, I.L., Carter, A., Flowerdew, M.J., Burton-Johnson, A., Bastias, J., Storey, C.D., Castillo, P., Chew, D., and Whitehouse, M.J., 2023, Evolution of an accretionary complex (LeMay Group) and terrane translation in the Antarctic Peninsula: Tectonics, v. 42, https://doi .org /10 .1029 /2022TC007578.
Robertson, A.H.F., Campbell, H.C., Johnston, M., and Mortimer, N., 2019, Introduction to Palaeozoic–Mesozoic geology of South Island, New Zealand: Subduction-related processes adjacent to SE Gondwana, *in* Robertson, A.H.F., ed., Palaeozoic–Mesozoic Geology of South Island, New Zealand: Subduction-Related Processes Adjacent to SE Gondwana: Geological Society, London, Memoir 49, p. 1–14, https://doi .org /10 .1144 /M49 .7.
Schwartz, T.M., Surpless, K.D., Colgan, J.P., Johnstone, S.A., and Holm-Denoma, C.S., 2021, Detrital zircon record of magmatism and sediment dispersal across the North American Cordilleran arc system 28–48°N: Earth-Science Reviews, v. 220, https://doi .org /10 .1016 /j .earscirev .2021 .103734.
Siddoway, C.S., Sass, L.C., III, and Esser, R.P., 2005, Kinematic history of the Marie Byrd Land terrane, West Antarctica: Direct evidence from Cretaceous mafic dykes, *in* Vaughan, A.P.M, Leat, P.T., and Pankhurst, R.J., eds., Terrane Processes at the Margins of Gondwana: Geological Society, London, Special Publication 246, p. 417–438.
Simões Pereira, P., van de Flierdt, T., Hemming, S.R., Hammond, S.J., Kuhn, G., Brachfeld, S., Doherty, C., and Hillenbrand, C.-D., 2018, Geochemical fingerprints of glacially eroded bedrock from West Antarctica: Detrital thermochronology, radiogenic isotope systematics and trace element geochemistry in Late Holocene glacial-marine sediments: Earth-Science Reviews, v. 182, p. 204–232, https://doi .org /10 .1016 /j .earscirev .2018 .04 .011.
Sláma, J., Košler, J., Condon, D.J., Crowley, J.L., Gerdes, A., Hanchar, J.M., Horstwood, M.S.A., Morris, G.A., Nasdala, L., Norberg, N., Schaltegger, U., Schoene, B., Tubrett, M.N., and Whitehouse, M.J., 2008, Plešovice zircon—A new natural reference material for U–Pb and Hf isotopic microanalysis: Chemical Geology, v. 249, p. 1–35, https://doi .org /10 .1016 /j .chemgeo .2007 .11 .005.
Smellie, J.L., 2021, Antarctic Peninsula—Geology and dynamic development, *in* Kleinschmidt, G., ed., Geology of the Antarctic Continent: Stuttgart, Germany, Gebrüder Borntraeger Verlagsbuchhandlung, p. 18–86.
Smellie, J.L., and Hole, M.J., 2021, Antarctic Peninsula: Volcanology, *in* Smellie, J.L., Panter, K.S., and Geyer, A., eds., Volcanism in Antarctica: 200 Million Years of Subduction, Rifting and Continental Break-up: Geological Society, London, Memoir 55, p. 305–325, https://doi .org /10 .1144 /M55-2018-59.
Söderlund, U., Patchett, P.J., Vervoort, J.D., and Isachsen, C.E., 2004, The $^{176}$Lu decay constant determined by Lu–Hf and U–Pb isotope systematics of Precambrian mafic intrusions: Earth and Planetary Science Letters, v. 219, p. 311–324, https://doi .org /10 .1016 /S0012 -821X(04)00012-3.
Stacey, J.S., and Kramers, J.D., 1975, Approximation of terrestrial lead evolution by a two-stage model: Earth and Planetary Science Letters, v. 26, p. 207–221, https://doi .org /10 .1016 /0012-821X(75)90088-6.
Storey, B.C., and Nell, P.A.R., 1988, Role of strike-slip faulting in the tectonic evolution of the Antarctic Peninsula: Journal of the Geological Society, v. 145, p. 333–337, https://doi .org /10 .1144 /gsjgs .145 .2.0333.
Storey, B.C., Brown, R.W., Carter, A., Doubleday, P.A., Hurford, A.J., Macdonald, D.I.M., and Nell, P.A.R., 1996, Fission-track evidence for the thermotectonic evolution of a Mesozoic–Cenozoic fore-arc, Antarctica: Journal of the Geological Society, v. 153, p. 65–82, https://doi .org /10 .1144 /gsjgs .153 .1.0065.

Surpless, K.D., Clemens-Knott, D., Barth, A.P., and Gevedon, M., 2019, A survey of Sierra Nevada magmatism using Great Valley detrital zircon trace-element geochemistry: View from the forearc: Lithosphere, v. 11, p. 603–619, https://doi .org /10 .1130 /L1059 .1.
Taylor, B.J., Thomson, M.R.A., and Willey, L.E., 1979, The geology of the Ablation Point-Keystone Cliffs area, Alexander Island: British Antarctic Survey: Scientific Reports, v. 82, p. 1–65.
Tranter, T.H., 1987, The structural history of the LeMay Group of central Alexander Island, Antarctica: British Antarctic Survey Bulletin, v. 74, p. 61–80.
Tranter, T.H., 1988, The tectonostratigraphic history of the LeMay Group of central Alexander Island, Antarctica [Ph.D. thesis]: Council for National Academic Awards, 272 p.
Trouw, R.A.J., Simoes, L.S.A., and Valladares, C., 1998, Metamorphic evolution of a subduction complex, South Shetland Islands, Antarctica: Journal of Metamorphic Geology, v. 16, p. 475–490, https://doi .org /10 .1111 /j .1525-1314 .1998 .00151 .x.
Twinn, G., Riley, T.R., Fox, M., and Carter, A., 2022, Thermal history of the southern Antarctic Peninsula during Cenozoic oblique subduction: Journal of the Geological Society, v. 179, https://doi .org /10 .1144 /jgs2022-008.
Vaughan, A.P.M., and Storey, B.C., 2000, The eastern Palmer Land shear zone: A new terrane accretion model for the Mesozoic development of the Antarctic Peninsula: Journal of the Geological Society, v. 157, p. 1243–1256, https://doi .org /10 .1144 /jgs .157 .6.1243.
Vaughan, A.P.M., Pankhurst, R.J., and Fanning, C.M., 2002, A mid-Cretaceous age for the Palmer Land event: Implications for terrane accretion timing and Gondwana palaeolatitudes: Journal of the Geological Society, v. 159, p. 113–116, https://doi .org /10 .1144 /0016 -764901-090.
Vaughan, A.P.M., Eagles, G., and Flowerdew, M.J., 2012, Evidence for a two-phase Palmer Land event from crosscutting structural relationships and emplacement timing of the Lassiter Coast Intrusive Suite, Antarctic Peninsula: Implications for mid-Cretaceous Southern Ocean plate configuration: Tectonics, v. 31, https://doi .org /10 .1029 /2011TC003006.
Velev, S., Lazarova, A., Karaoglan, F., Vassilev, O., and Selbesoğlu, M.O., 2023, Early Jurassic and Late Cretaceous magmatism on Horseshoe Island, Antarctic Peninsula: New U-Pb and microstructural data: Geologica Balcanica, v. 52, no. 3, p. 29–32, https://doi .org /10 .52321 /GeolBalc .52 .3.29.
Vermeesch, P., 2018, IsoplotR: A free and open toolbox for geochronology: Geoscience Frontiers, v. 9, p. 1479–1493, https://doi .org /10 .1016 /j .gsf .2018 .04 .001.
Whitehouse, M.J., and Kamber, B.S., 2005, Assigning dates to thin gneissic veins in high-grade metamorphic terranes: A cautionary tale from Akilia, southwest Greenland: Journal of Petrology, v. 46, p. 291–318, https://doi .org /10 .1093 /petrology /egh075.

**Figure Captions**

Figure 1. Geological map of the Antarctic Peninsula (after Burton-Johnson and Riley, 2015). AP—Antarctic Peninsula; TI—Thurston Island; MBL—Marie Byrd Land; PLSZ—Palmer Land shear zone; WD—Western Domain; CD—Central Domain; ED—Eastern Domain (Vaughan and Storey, 2000). Core sites in the Amundsen Sea region (see inset) are from Simões Pereira et al. (2018). Maps were generated in QGIS geographic information system software.

Figure 2. Geological map of Alexander Island showing the main lithological units. Approxi- mate positions of the Fossil Bluff Group sample sites are also shown. More precise localities are shown in Figure 3, and exact positions are shown in Table S1.

Figure 3. Updated geological map of the Fossil Bluff Group showing detailed sample sites and the major units (from Butterworth et al., 1988; Crame and Howlett, 1988; Doubleday et al., 1993; Moncrieff and Kelly, 1993; Nichols and Cantrill, 2002).

Figure 4. Relative probability density plots of U-Pb detrital zircon ages for a range of sandstone–siltstone–conglomerate lithologies from the Fossil Bluff Group forearc basin. Kernel density estimator curves are shown as red dashed lines. Full datasets are available in Table S2 (see text footnote 1). Binwidths for all plotted samples are 20 Ma.

Figure 5. U-Pb zircon ages (238U/206Pb) versus initial εHf values for zircon grains analyzed in this study (Table S3; see text footnote 1). (A) Fossil Bluff Group forearc basin (this study). Comparative units are from 1—Riley et al. (2020a), 2—Bastias et al. (2023), 3—Riley et al. (2023), 4—British Antarctic Survey unpublished data, and 5—Nelson and Cottle (2018). (B) Latady Group, Botany Bay Group, and Mount Hill Formation (Riley et al., 2023). (C) LeMay Group accretionary complex (Riley et al., 2023). Geochemical envelopes for Marie Byrd Land and Antarctic Peninsula/Thurston Island are from Nelson and Cottle (2018). CHUR—chondritic uniform reservoir.

Figure 6. Multidimensional scaling (MDS) maps (Vermeesch, 2018) comparing the age spectra in dissimilar samples were calculated using the Kolmogorov-Smirnov statistic. MDS plots map the degree of similarity between each sample, with any two points plotting closer if they are more similar. Axis scales are dimensionless and have no physical meaning. MDS plot in this figure shows ages younger than 600 Ma from the Fossil Bluff Group (this study). Age populations older than 600 Ma are essentially absent (see Fig. 4), and hence were excluded. Sample locations are shown in Figure 3, where the unit numbers are defined in the stratigraphy. U-Pb zircon data used for MDS analysis are presented in Table S2 (see text footnote 1). All comparative data are from Riley et al. (2023), and the locations of lithological units are shown in Figure 1

Figure 7. Probability density plot showing the distribution of all Jurassic–Cretaceous ages from the Fossil Bluff Group and the calculated rates for convergence of the Aluk (Phoenix) Plate with the Antarctic Peninsula (Riley et al., 2020a). Magmatic and tectonic events are from Pankhurst et al. (2000), Riley et al. (2018, 2020a), and Bastias et al. (2023).

Figure 8. Kinematic GPlates reconstruction for the (A) Middle Jurassic and (B) mid-Cretaceous. Adapted from Riley et al. (2023). Yellow arrows depict potential sediment transport.

**Figures**

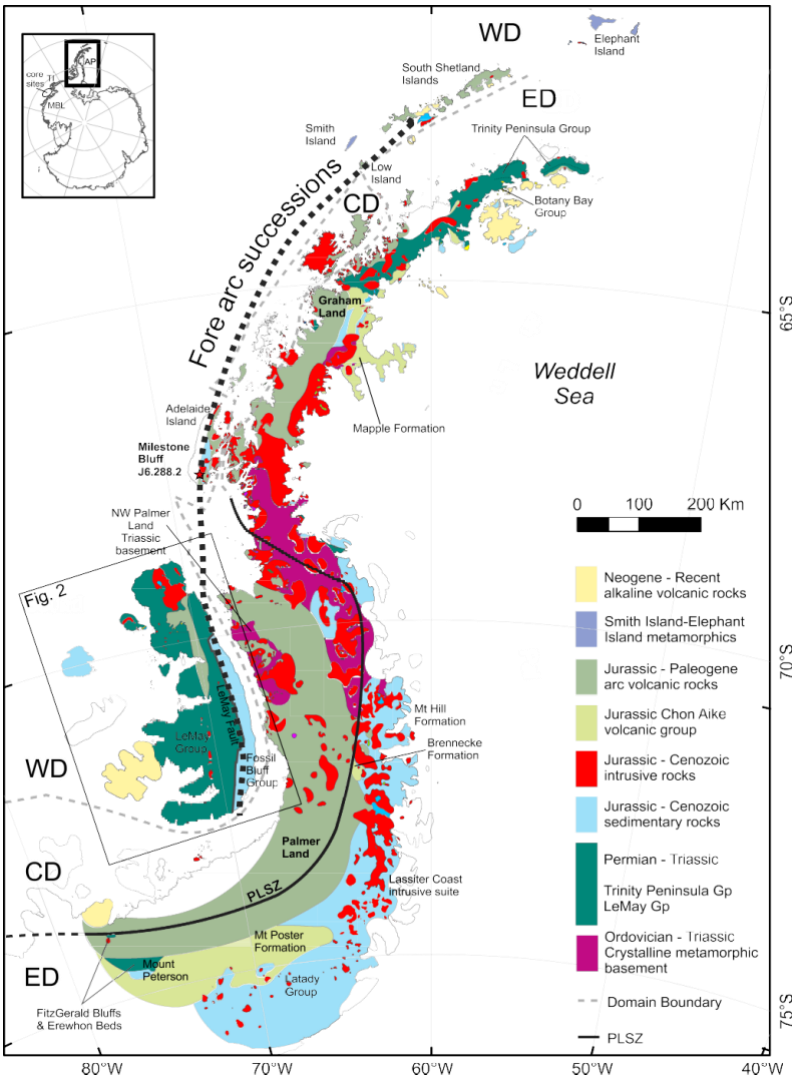
WD
Elephant Island
South Shetland Islands
ED
Smith Island
Trinity Peninsula Group
Low Island
CD
Botany Bay Group
Fore arc successions
Graham Land
Weddell Sea
Adelaide Island
Mapple Formation
Milestone Bluff J6.288.2
NW Palmer Land Triassic basement
Fig. 2
LeMay Fault
LeMay Group
Fossil Bluff Group
Mt Hill Formation
Brennecke Formation
WD
Palmer Land
CD
PLSZ
Lassiter Coast intrusive suite
Mt Poster Formation
Mount Peterson
Latady Group
ED
FitzGerald Bluffs & Erewhon Beds
0 100 200 Km
Neogene - Recent alkaline volcanic rocks
Smith Island-Elephant Island metamorphics
Jurassic - Paleogene arc volcanic rocks
Jurassic Chon Aike volcanic group
Jurassic - Cenozoic intrusive rocks
Jurassic - Cenozoic sedimentary rocks
Permian - Triassic
Trinity Peninsula Gp
LeMay Gp
Ordovician - Triassic Crystalline metamorphic basement
Domain Boundary
PLSZ
65°S
70°S
75°S
80°W
70°W
60°W
50°W
40°W

Fig. 1

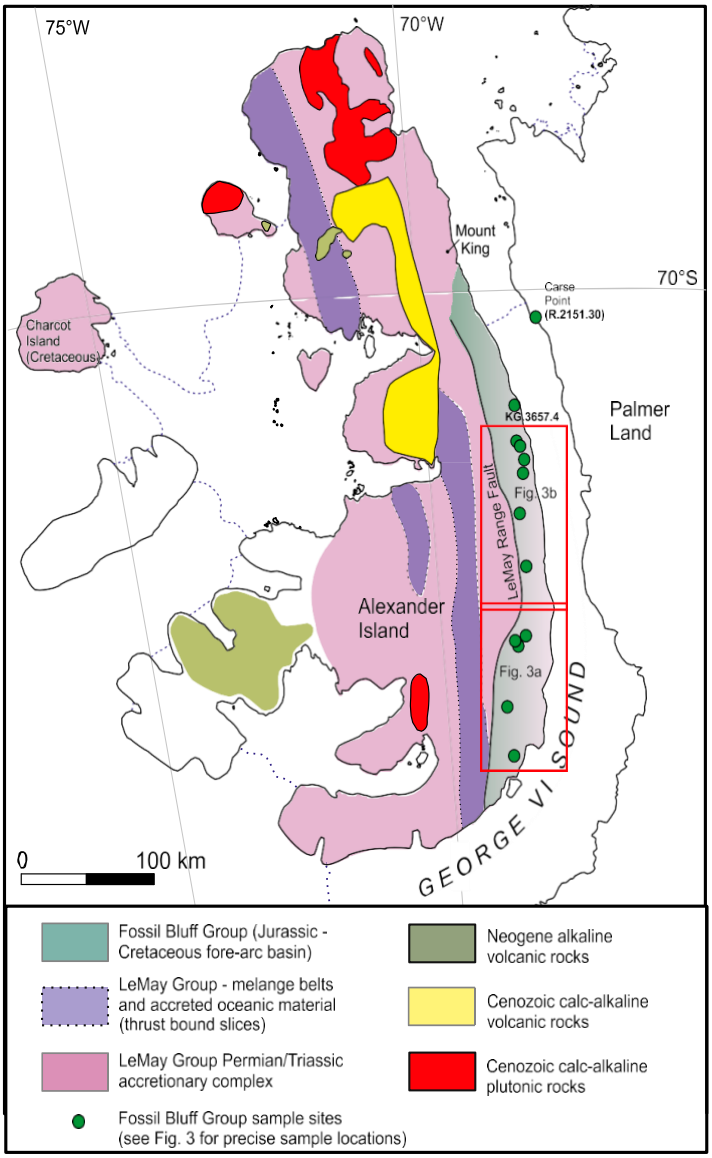
75°W
70°W
70°S
Mount King
Carse Point (R.2151.30)
Charcot Island (Cretaceous)
KG.3657.4
Palmer Land
LeMay Range Fault
Fig. 3b
Fig. 3a
Alexander Island
GEORGE VI SOUND
0
100 km
Fossil Bluff Group (Jurassic - Cretaceous fore-arc basin)
LeMay Group - melange belts and accreted oceanic material (thrust bound slices)
LeMay Group Permian/Triassic accretionary complex
Fossil Bluff Group sample sites (see Fig. 3 for precise sample locations)
Neogene alkaline volcanic rocks
Cenozoic calc-alkaline volcanic rocks
Cenozoic calc-alkaline plutonic rocks

Fig. 2

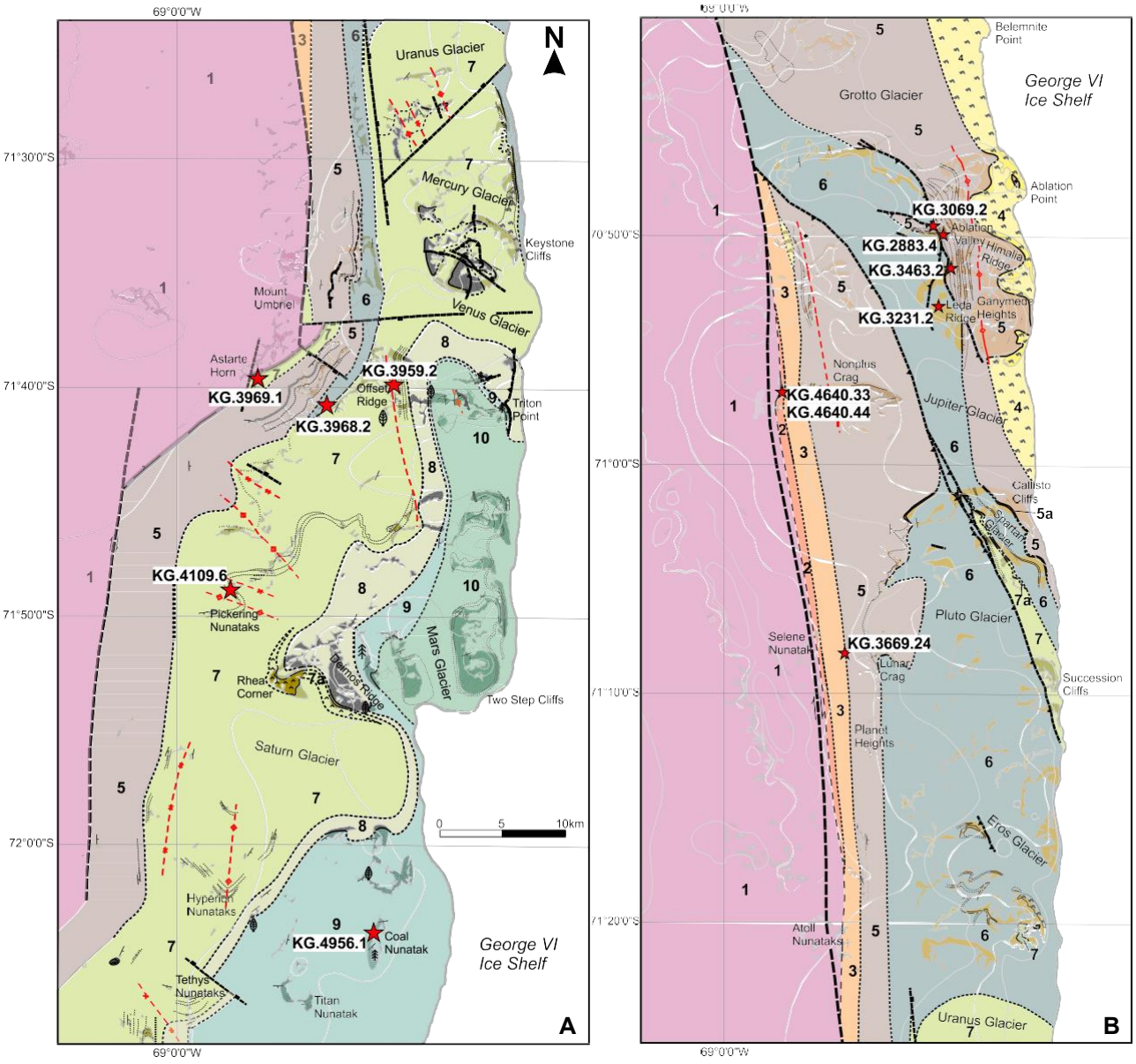
69°0'0"W
71°30'0"S
71°40'0"S
71°50'0"S
72°0'0"S
N
Uranus Glacier
Mercury Glacier
Venus Glacier
Keystone Cliffs
Mount Umbriel
Astarte Horn
KG.3969.1
KG.3959.2
Offset Ridge
KG.3968.2
Triton Point
KG.4109.6
Pickering Nunataks
Rhea Corner
Deimos Ridge
Mars Glacier
Two Step Cliffs
Saturn Glacier
0 5 10km
Hyperion Nunataks
KG.4956.1
Coal Nunatak
Tethys Nunataks
Titan Nunatak
George VI Ice Shelf
A
Belemnite Point
Grotto Glacier
George VI Ice Shelf
Ablation Point
KG.3069.2
Ablation Valley
KG.2883.4
Himalia Ridge
KG.3463.2
Leda Ridge
Ganymede Heights
KG.3231.2
Nonplus Crag
KG.4640.33
KG.4640.44
Jupiter Glacier
70°50'0"S
71°0'0"S
71°10'0"S
71°20'0"S
Callisto Cliffs
5a
Spartan Glacier
Pluto Glacier
Selene Nunatak
KG.3669.24
Lunar Crag
Succession Cliffs
Planet Heights
Eros Glacier
Atoll Nunataks
Uranus Glacier
B

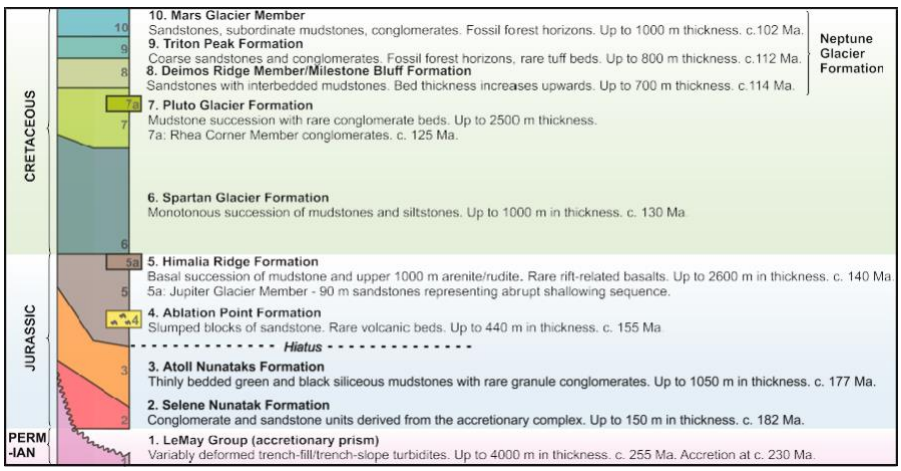
CRETACEOUS
JURASSIC
PERM-IAN
10. Mars Glacier Member
Sandstones, subordinate mudstones, conglomerates. Fossil forest horizons. Up to 1000 m thickness. c.102 Ma.
9. Triton Peak Formation
Coarse sandstones and conglomerates. Fossil forest horizons, rare tuff beds. Up to 800 m thickness. c.112 Ma.
8. Deimos Ridge Member/Milestone Bluff Formation
Sandstones with interbedded mudstones. Bed thickness increases upwards. Up to 700 m thickness. c.114 Ma.
Neptune Glacier Formation
7. Pluto Glacier Formation
Mudstone succession with rare conglomerate beds. Up to 2500 m thickness.
7a: Rhea Corner Member conglomerates. c. 125 Ma.
6. Spartan Glacier Formation
Monotonous succession of mudstones and siltstones. Up to 1000 m in thickness. c. 130 Ma
5. Himalia Ridge Formation
Basal succession of mudstone and upper 1000 m arenite/rudite. Rare rift-related basalts. Up to 2600 m in thickness. c. 140 Ma
5a: Jupiter Glacier Member - 90 m sandstones representing abrupt shallowing sequence.
4. Ablation Point Formation
Slumped blocks of sandstone. Rare volcanic beds. Up to 440 m in thickness. c. 155 Ma
Hiatus
3. Atoll Nunataks Formation
Thinly bedded green and black siliceous mudstones with rare granule conglomerates. Up to 1050 m in thickness. c. 177 Ma.
2. Selene Nunatak Formation
Conglomerate and sandstone units derived from the accretionary complex. Up to 150 m in thickness. c. 182 Ma.
1. LeMay Group (accretionary prism)
Variably deformed trench-fill/trench-slope turbidites. Up to 4000 m in thickness. c. 255 Ma. Accretion at c. 230 Ma.

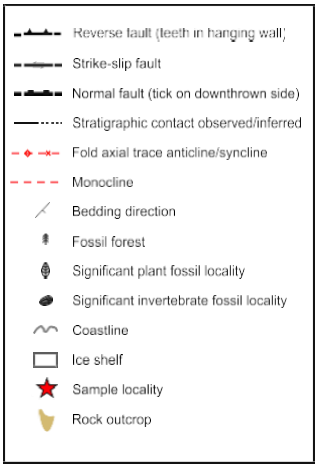
Reverse fault (teeth in hanging wall)
Strike-slip fault
Normal fault (tick on downthrown side)
Stratigraphic contact observed/inferred
Fold axial trace anticline/syncline
Monocline
Bedding direction
Fossil forest
Significant plant fossil locality
Significant invertebrate fossil locality
Coastline
Ice shelf
Sample locality
Rock outcrop

Fig. 3

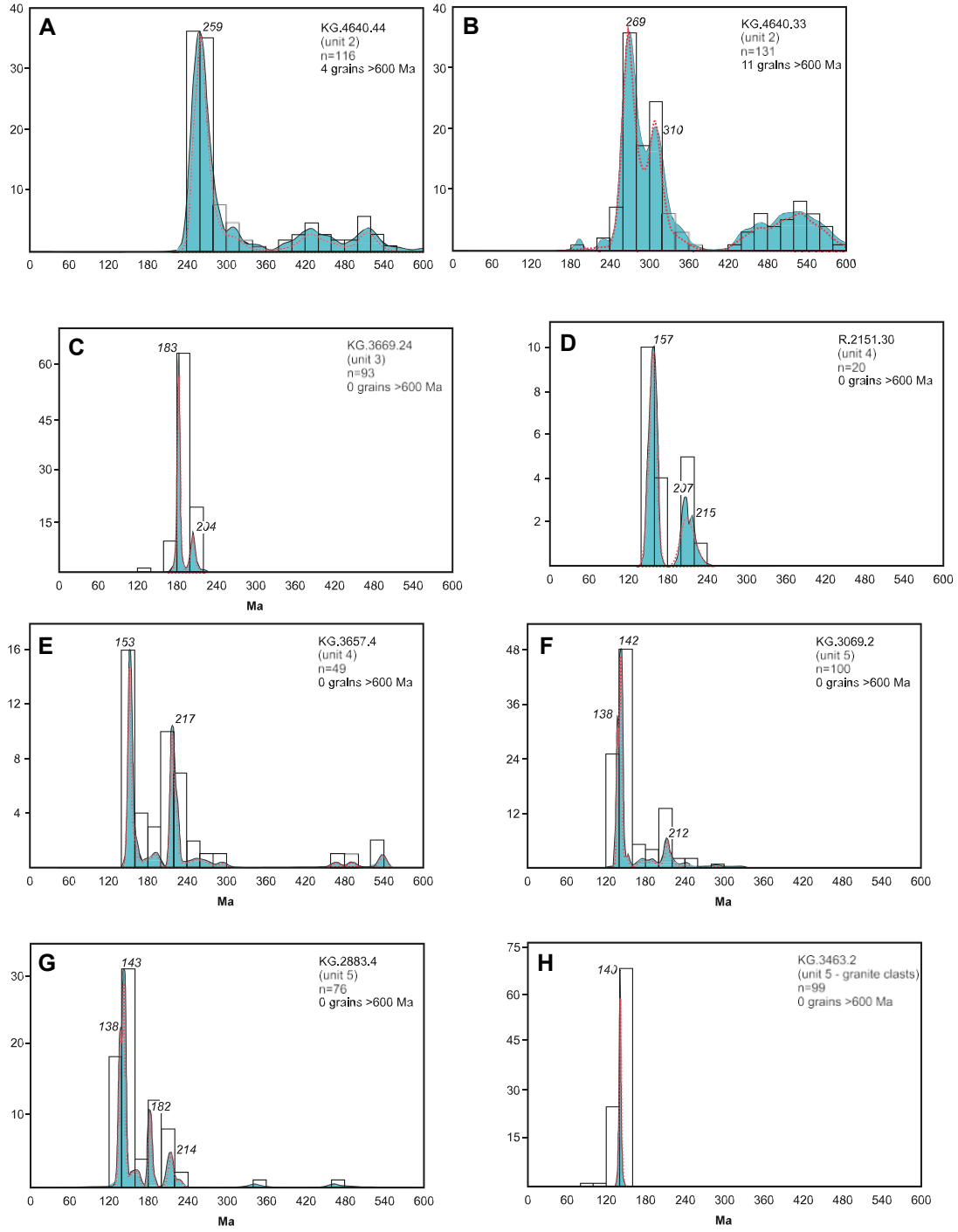
A
259
KG.4640.44
(unit 2)
n=116
4 grains >600 Ma
B
269
310
KG.4640.33
(unit 2)
n=131
11 grains >600 Ma
C
183
204
KG.3669.24
(unit 3)
n=93
0 grains >600 Ma
D
157
207
215
R.2151.30
(unit 4)
n=20
0 grains >600 Ma
E
153
217
KG.3657.4
(unit 4)
n=49
0 grains >600 Ma
F
142
138
212
KG.3069.2
(unit 5)
n=100
0 grains >600 Ma
G
143
138
182
214
KG.2883.4
(unit 5)
n=76
0 grains >600 Ma
H
140
KG.3463.2
(unit 5 - granite clasts)
n=99
0 grains >600 Ma
Ma

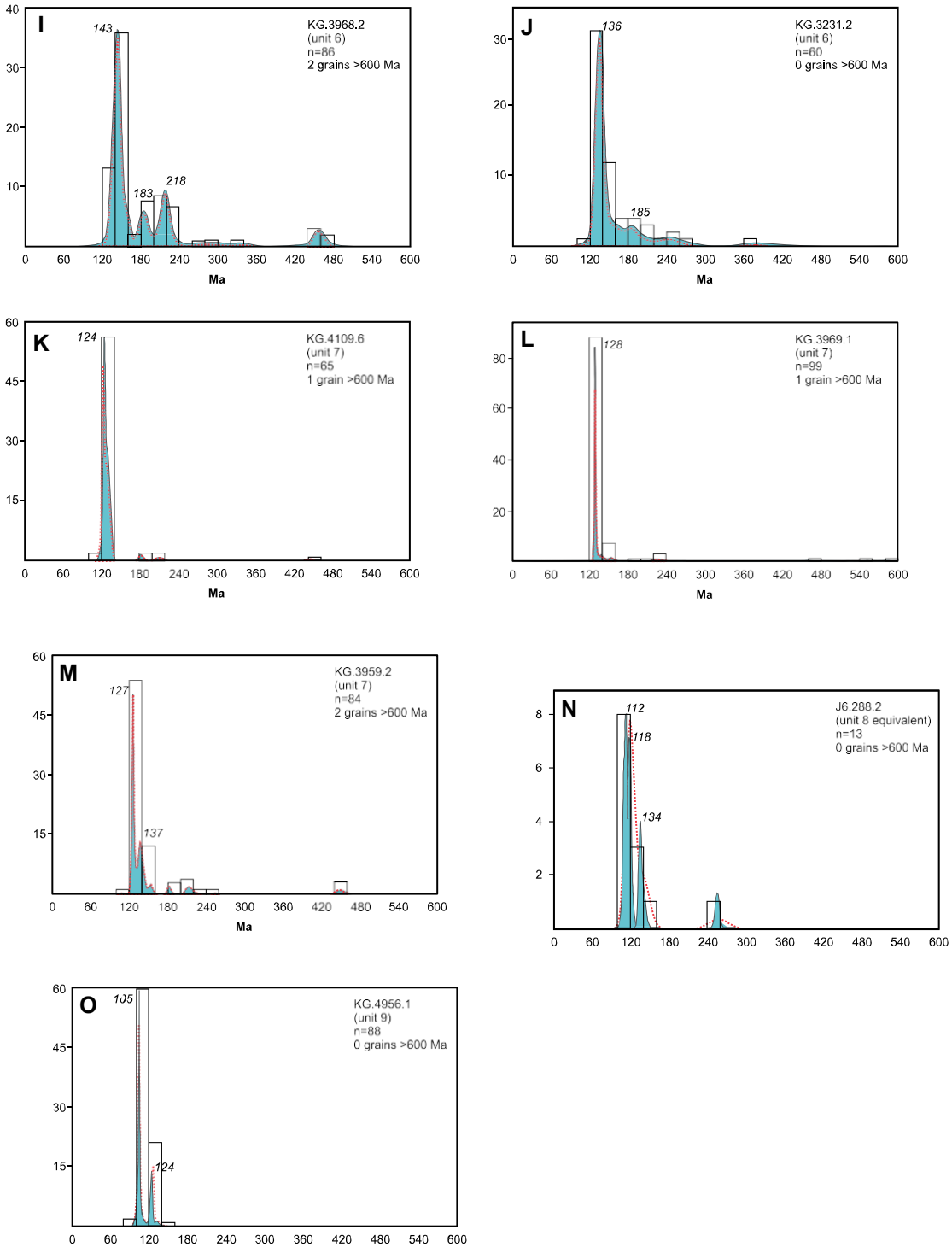
I
KG.3968.2
(unit 6)
n=86
2 grains >600 Ma
143
183
218
J
KG.3231.2
(unit 6)
n=60
0 grains >600 Ma
136
185
K
KG.4109.6
(unit 7)
n=65
1 grain >600 Ma
124
L
KG.3969.1
(unit 7)
n=99
1 grain >600 Ma
128
M
KG.3959.2
(unit 7)
n=84
2 grains >600 Ma
127
137
N
J6.288.2
(unit 8 equivalent)
n=13
0 grains >600 Ma
112
118
134
O
KG.4956.1
(unit 9)
n=88
0 grains >600 Ma
105
124
Ma

Fig. 4

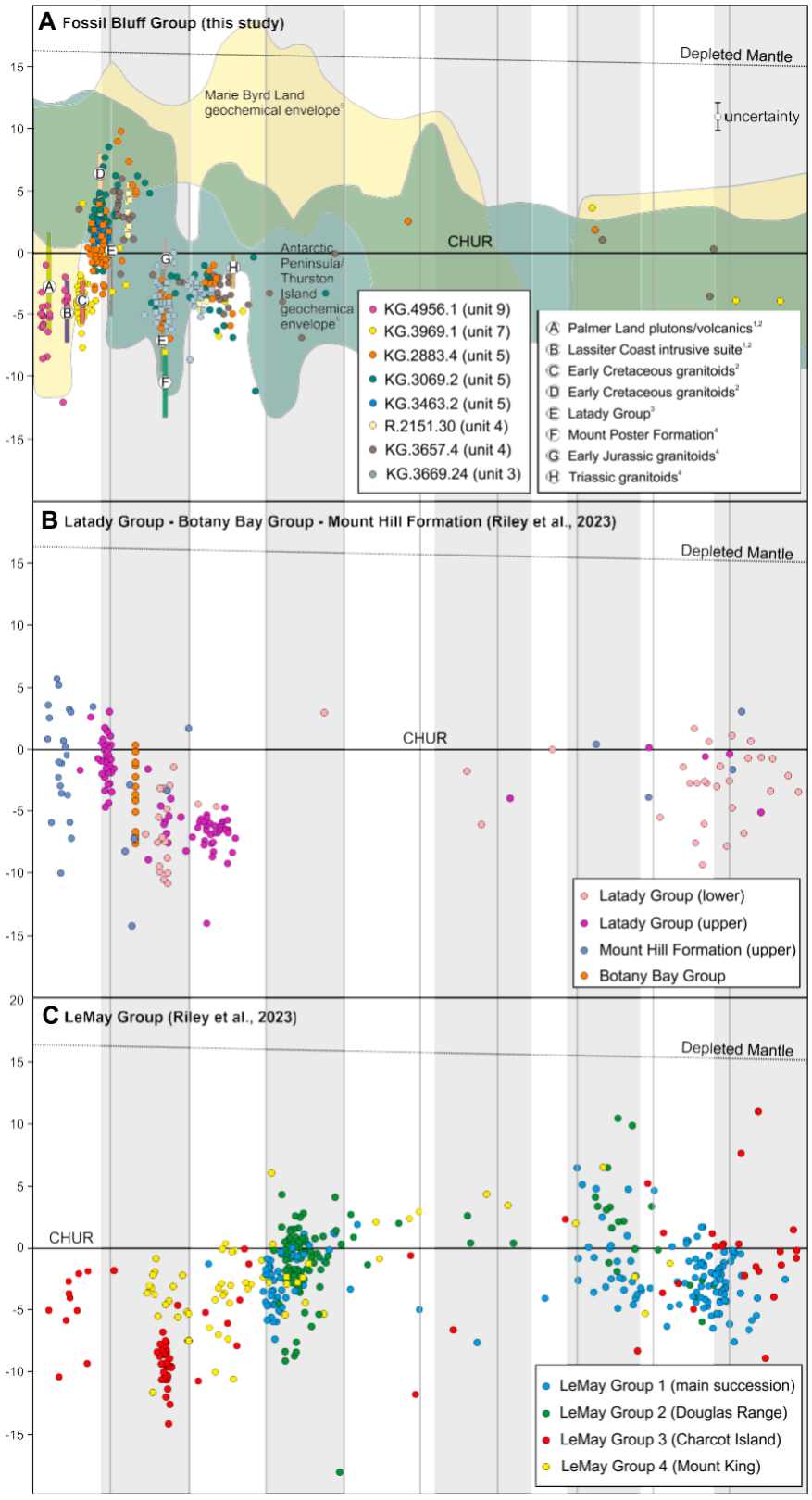
A Fossil Bluff Group (this study)
Depleted Mantle
Marie Byrd Land geochemical envelope
uncertainty
CHUR
Antarctic Peninsula/ Thurston Island geochemical envelope
KG.4956.1 (unit 9)
KG.3969.1 (unit 7)
KG.2883.4 (unit 5)
KG.3069.2 (unit 5)
KG.3463.2 (unit 5)
R.2151.30 (unit 4)
KG.3657.4 (unit 4)
KG.3669.24 (unit 3)
A Palmer Land plutons/volcanics
B Lassiter Coast intrusive suite
C Early Cretaceous granitoids
D Early Cretaceous granitoids
E Latady Group
F Mount Poster Formation
G Early Jurassic granitoids
H Triassic granitoids
B Latady Group - Botany Bay Group - Mount Hill Formation (Riley et al., 2023)
Depleted Mantle
CHUR
Latady Group (lower)
Latady Group (upper)
Mount Hill Formation (upper)
Botany Bay Group
C LeMay Group (Riley et al., 2023)
Depleted Mantle
CHUR
LeMay Group 1 (main succession)
LeMay Group 2 (Douglas Range)
LeMay Group 3 (Charcot Island)
LeMay Group 4 (Mount King)

Fig. 5

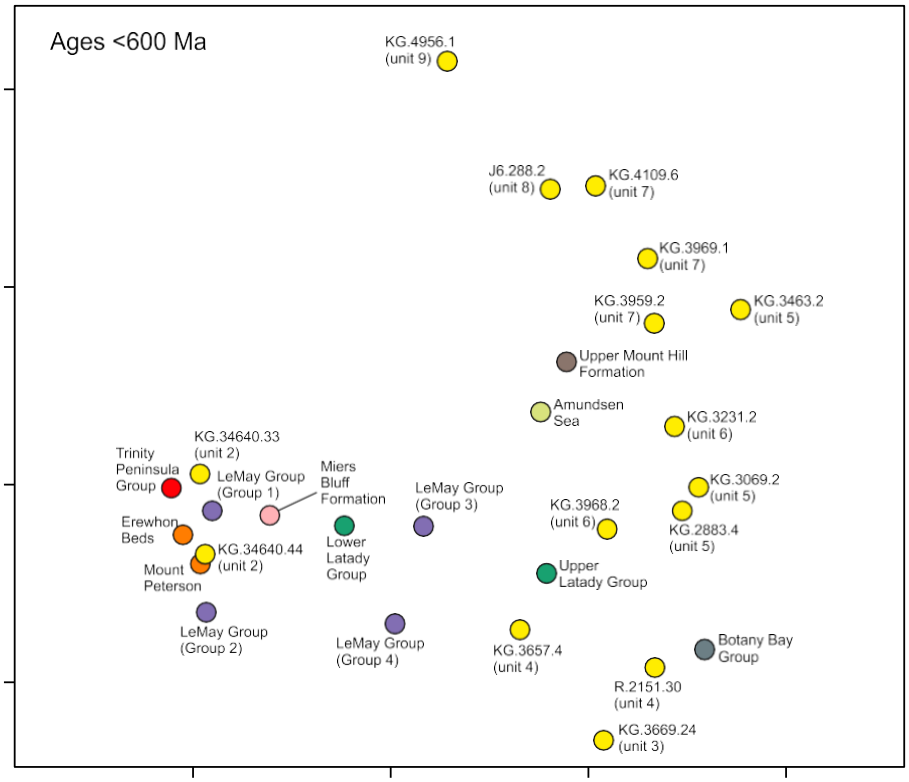
Ages <600 Ma
KG.4956.1
(unit 9)
J6.288.2
(unit 8)
KG.4109.6
(unit 7)
KG.3969.1
(unit 7)
KG.3959.2
(unit 7)
KG.3463.2
(unit 5)
Upper Mount Hill
Formation
Amundsen
Sea
KG.3231.2
(unit 6)
KG.34640.33
(unit 2)
Trinity
Peninsula
Group
LeMay Group
(Group 1)
Miers
Bluff
Formation
LeMay Group
(Group 3)
KG.3069.2
(unit 5)
KG.3968.2
(unit 6)
KG.2883.4
(unit 5)
Erewhon
Beds
Lower
Latady
Group
KG.34640.44
(unit 2)
Mount
Peterson
Upper
Latady Group
LeMay Group
(Group 2)
LeMay Group
(Group 4)
KG.3657.4
(unit 4)
Botany Bay
Group
R.2151.30
(unit 4)
KG.3669.24
(unit 3)

Fig. 6

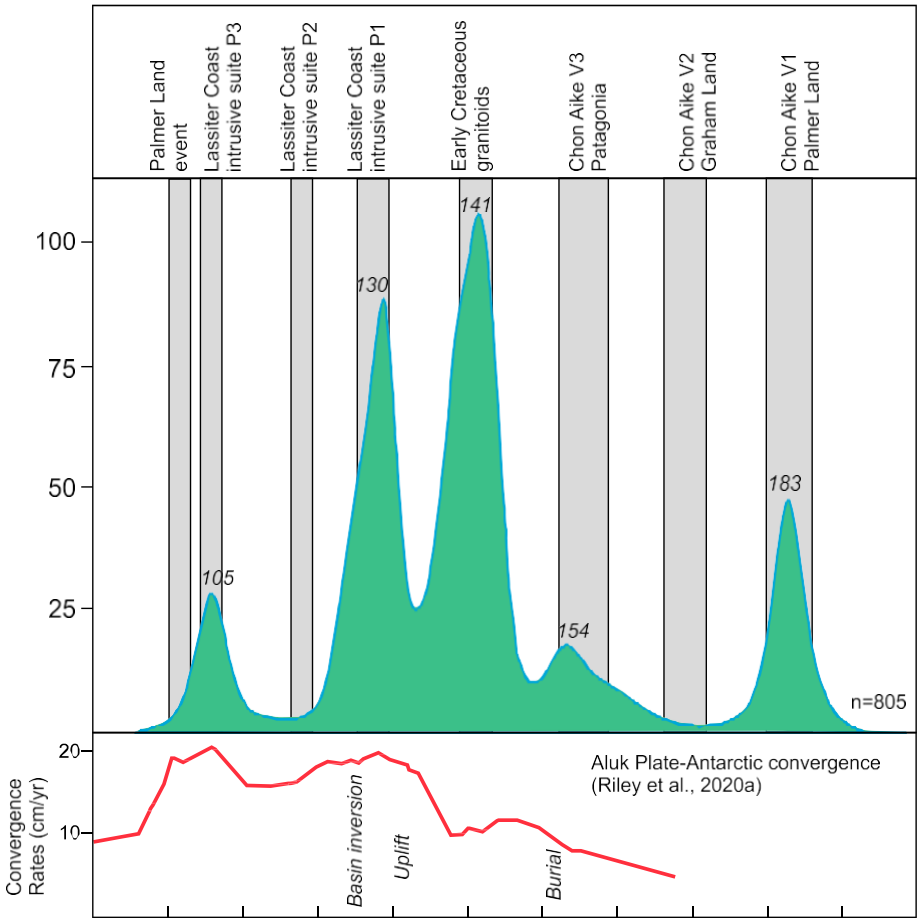
Palmer Land event
Lassiter Coast intrusive suite P3
Lassiter Coast intrusive suite P2
Lassiter Coast intrusive suite P1
Early Cretaceous granitoids
Chon Aike V3 Patagonia
Chon Aike V2 Graham Land
Chon Aike V1 Palmer Land
100
75
50
25
105
130
141
154
183
n=805
20
10
Convergence Rates (cm/yr)
Aluk Plate-Antarctic convergence (Riley et al., 2020a)
Basin inversion
Uplift
Burial

Fig. 7

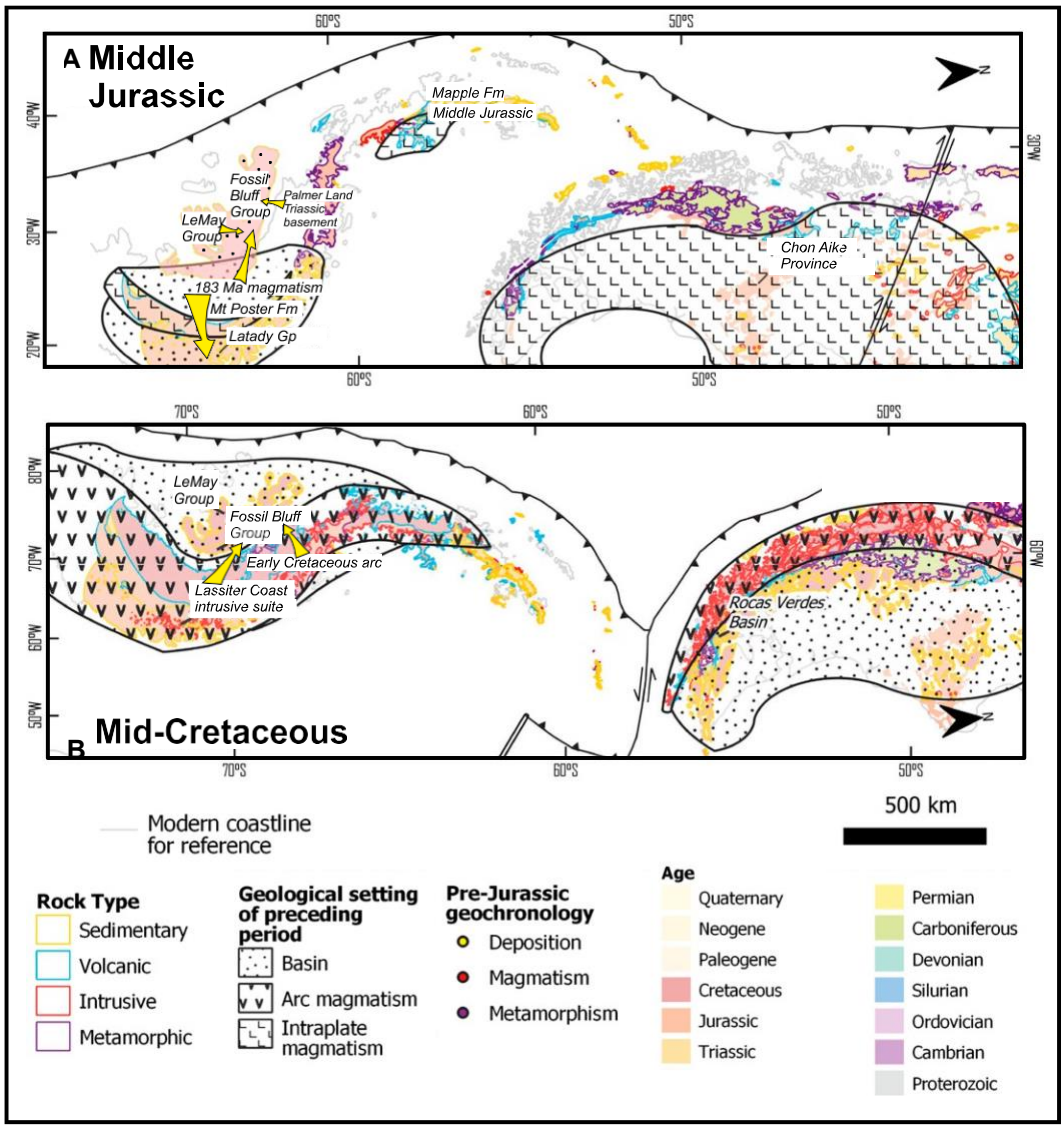
A Middle Jurassic
Mapple Fm
Middle Jurassic
Fossil Bluff Group
Palmer Land Triassic basement
LeMay Group
183 Ma magmatism
Mt Poster Fm
Latady Gp
Chon Aike Province
B Mid-Cretaceous
LeMay Group
Fossil Bluff Group
Early Cretaceous arc
Lassiter Coast intrusive suite
Rocas Verdes Basin
60°S
50°S
70°S
30°W
40°W
60°W
80°W
Modern coastline for reference
500 km
Rock Type
Sedimentary
Volcanic
Intrusive
Metamorphic
Geological setting of preceding period
Basin
Arc magmatism
Intraplate magmatism
Pre-Jurassic geochronology
Deposition
Magmatism
Metamorphism
Age
Quaternary
Neogene
Paleogene
Cretaceous
Jurassic
Triassic
Permian
Carboniferous
Devonian
Silurian
Ordovician
Cambrian
Proterozoic

Fig. 8